arXiv:2302.03322v2 [cs.LG] 11 Jun 2023

Attacking Cooperative Multi-Agent Reinforcement Learning by Adversarial Minority Influence

Simin Li, Jun Guo, Jingqiao Xiu, Pu Feng, Xin Yu, Jiakai Wang, Aishan Liu, Wenjun Wu, Xianglong Liu†

***Abstract*—This study probes the vulnerabilities of cooperative multi-agent reinforcement learning (c-MARL) under adversarial attacks, a critical determinant of c-MARL's worst-case performance prior to real-world implementation. Current observation-based attacks, constrained by white-box assumptions, overlook c-MARL's complex *multi-agent* interactions and *cooperative* objectives, resulting in impractical and limited attack capabilities. To address these shortcomes, we propose *Adversarial Minority Influence* (AMI), a practical and strong for c-MARL. AMI is a practical black-box attack and can be launched without knowing victim parameters. AMI is also strong by considering the complex *multi-agent* interaction and the *cooperative* goal of agents, enabling a single adversarial agent to *unilaterally* misleads majority victims to form *targeted* worst-case cooperation. This mirrors minority influence phenomena in social psychology. To achieve maximum deviation in victim policies under complex agent-wise interactions, our *unilateral* attack aims to characterize and maximize the impact of the adversary on the victims. This is achieved by adapting a unilateral agent-wise relation metric derived from mutual information, thereby mitigating the adverse effects of victim influence on the adversary. To lead the victims into a jointly detrimental scenario, our *targeted* attack deceives victims into a long-term, cooperatively harmful situation by guiding each victim towards a specific target, determined through a trial-and-error process executed by a reinforcement learning agent. Through AMI, we achieve the first successful attack against real-world robot swarms and effectively fool agents in simulated environments into collectively worst-case scenarios, including Starcraft II and Multi-agent Mujoco. The source code and demonstrations can be found at: https://github.com/DIG-Beihang/AMI.**

***Index Terms*—Multi-agent reinforcement learning, trustworthy reinforcement learning, adversarial attack, algorithmic testing.**

I. Introduction

COOPERATIVE multi-agent reinforcement learning (c-MARL) involves the coordination of multiple agents, each employing individual policies to attain a common objective within an environment, based on their respective observations. Despite facing numerous distinct challenges, such as combinatorial action complexity, partial observation, credit assignment, and non-stationarity [1]–[4], contemporary state-of-the-art c-MARL algorithms have demonstrated encouraging results in various real-world applications. These encompass cooperative gaming [5], traffic light management [6], distributed resource allocation [7], [8], and cooperative swarm control [9]–[11].

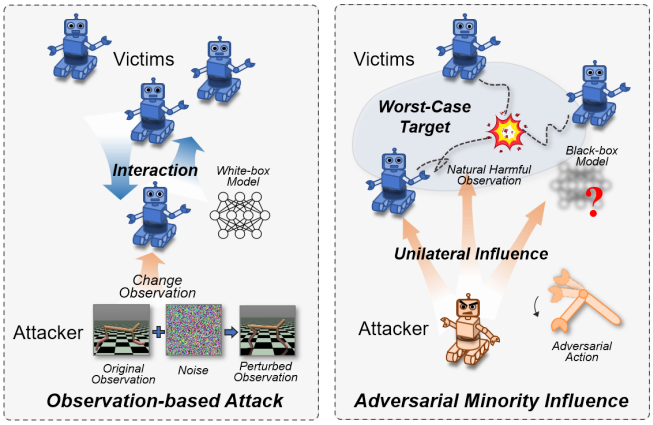

Fig. 1: A comparison of various attack methodologies in c-MARL. Observation-based attacks necessitate white-box access to the agent model and impose unrealistic pixel-wise perturbations on agent observations. In contrast, our proposed adversarial minority influence approach represents a policy-based attack that allows a single minority attacker to execute legitimate actions, thereby unilaterally directing the majority of victims toward a mutually detrimental target.

While c-MARL has achieved notable success, research has exposed the vulnerability of c-MARL agents to observation-based adversarial attacks [12], wherein adversaries introduce perturbations to an agent's observation, causing it to execute suboptimal actions. Given the interrelated nature of victim actions for cooperation, other c-MARL agents may become disoriented and being non-robust (see Fig. 1). As c-MARL algorithms frequently feature in security-sensitive applications, assessing their worst-case performance against potential adversarial interference is crucial before real world deployment. However, existing observation-based attacks depend on white-box access to the agent model and complete control of agent observations, rendering them highly impractical. For instance, in autonomous driving scenarios, it can be prohibitively hard for attackers to access the architectures, weights, and gradients utilized by a vehicle or to introduce arbitrary pixel-wise manipulations to camera input at each timestep [12]–[14].

In this paper, we take a practical and black-box alternative by conducting the first *policy-based adversarial attack* (i.e., *adversarial policy) [15]–[17] to assess the robustness of c-MARL*. Unlike direct observation manipulation, policy-based attacks perturb observations in a natural manner by incorporating an adversarial agent within the c-MARL environment—a

S. Li, J. Guo, J. Xiu, P. Feng, X. Yu, A. Liu and X. Liu are with the State Key Lab of Software Development Environment, Beihang University, Beijing 100191, China. J. Wang and X. Liu is with Zhongguancun Laboratory, Beijing, China. X. Liu is also with Institute of data space, Hefei Comprehensive National Science Center, Hefei, China. † Corresponding author: Xianglong Liu, xlliu@buaa.edu.cn.

Manuscript received June 10, 2023.

feasible approach in numerous c-MARL applications. For instance, adversaries can legitimately participate in distributed resource allocation clusters as individual workers [7], [18]–[20] or control their own vehicles while interacting with other vehicles in autonomous driving [21]–[24]. By interacting with the environment, the adversary learns an adversarial policy that directs it to execute physically plausible actions, which in turn adversely influence the observations of victim agents.

Although policy-based attacks have been investigated in two-agent competitive games [15]–[17], these studies have neglected two crucial challenges in c-MARL, resulting in diminished attack efficacy. Ideally, the adversary should *influence* victims toward a *cooperatively* inferior policy. This gives rise to two issues: (1) The *influence* problem, wherein all agents mutually influence one another in c-MARL; consequently, attacking a single victim impacts the policies of other victims as well. In the face of such intricate agent-wise influence, it becomes difficult for the adversary to maximally deviate victim policies and identify the optimal attack strategy. (2) The *cooperation* problem, which arises as merely perturbing victim actions arbitrarily or toward locally suboptimal cases is insufficient to indicate the failure of cooperative victims. The adversary faces the challenge of exploring and deceiving victims into a long-term, jointly detrimental failure scenario.

To address the aforementioned challenges, we introduce *Adversarial Minority Influence (AMI)*, the first adversarial policy attack designed for c-MARL. As depicted in Fig. 1, AMI distinguishes itself from other attacks by deceiving victims in an *unilateral* and *targeted* manner. The term *minority influence* originates from social psychology [25], wherein a resolute minority (adversary) can *unilaterally* sway majorities (victims) to adopt its own *targeted* belief. Technically, to maximally deviate victim policies amidst complex agent interactions, we quantify and maximize the adversarial impact from the adversary to each victim. Our *unilateral influence filter* adapts mutual information, a bilateral agent-wise relation metric, into a unilateral relation metric that represents the influence from the adversary to the victim. This is achieved by decomposing mutual information and filtering out the harmful influence from victims to the adversary. To deceive victims into a jointly worst-case failure, we guide each victim toward their own target, which collectively results in a long-term, worst-case failure. The target is determined by the *targeted adversarial oracle*, a reinforcement learning agent that generates worst-case target actions for each victim by co-adapting with our adversarial policy. Ultimately, the attacker modifies its policy to direct victims toward these adversarial target actions through unilateral influence. Our **contributions** are listed as follows:

- We develop AMI, a strong and practical attack towards c-MARL, which adeptly addresses the intricate influence among agents and effectively manages the cooperative nature of victims in c-MARL.
- We introduce the *unilateral influence filter* and *targeted adversarial oracle* to optimize the deviation of victim policies and deceive victims into suboptimal cooperation, thereby ensuring a potent attack capability.
- AMI achieves the first successful attack against real world robot swarms and effectively fool agents in simulation environments into collectively worst-case scenarios, including StarCraft II and Multi-agent Mujoco.

II. Related Work

A. Overview of Adversarial Attacks

Initially proposed in the field of computer vision, adversarial attacks consist of carefully crafted perturbations that, while imperceptible to humans, can deceive deep neural networks (DNNs) into making incorrect predictions [26]–[28]. Given a DNN F_θ, a clean image $\mathbf{x}$, a perturbed image $\mathbf{x}_{adv}$, and the ground truth label y, an adversarial example can be formulated as follows:

$$\mathbb{F}_\theta\left(x_{adv}\right) \neq y \quad s.t. \quad \|\mathbf{x}-\mathbf{x}_{adv}\| \leq \epsilon, \tag{1}$$

In this formulation, $\|\cdot\|$ represents a distance metric used to constrain the distance between $\mathbf{x}$ and $\mathbf{x}_{adv}$ by ϵ. Subsequently, it was demonstrated that reinforcement learning (RL) is also susceptible to adversarial attacks [13], [29], [30]. Owing to the sequential decision-making nature of RL, adversarial attacks in this context aim to generate a perturbation policy π^α that minimizes the victim's cumulative reward $\sum_t \gamma^t r_t$, which can be expressed as:

$$\min_{\pi^\alpha} \sum_t \gamma^t r_t. \tag{2}$$

Adversarial attacks are important to distinguish as test-time attacks, where the adversary targets a specific victim without participating in the training process. In contrast, training-time attacks interfere with victim training, resulting in trained victims either failing to perform well (poisoning attack) [31]–[33] or executing adversary-specified actions when specific triggers are present (backdoor attack) [34]–[37]. Training-time attacks can be carried out by modifying observations [34], [36], [37], trajectories [33], [35], or rewards [31], [32]. Note that our Adversarial Minority Influence (AMI) approach constitutes a test-time attack, and is not related to training-time attacks.

B. RL Attacks by Observation Perturbation

Test-time perturbation of RL observations can deceive the policy network of RL agents, causing them to execute suboptimal actions and fail to achieve their goals. For single-agent RL attacks, early research employed heuristics such as preventing victims from selecting the best action [13] or choosing actions with the lowest value at critical time steps [29], [30]. Later work framed the adversary and victim within an MDP structure [14], enabling the optimal observation perturbation to be learned as an action within the current state using an RL agent [38], [39]. For c-MARL attacks, Lin et al. [12] proposed a two-step attack that first learns a worst-case attack policy and then employs a gradient-based attack [27], [40] to execute it. However, this approach assumes the attacker can modify victim observations and possesses white-box access to victim parameters, which may be impractical in real-world scenarios. Another line of research, termed adversarial

communication, targets communicative c-MARL by focusing on sending messages to victim agents that cause failure upon receiving the adversarial message. Adversarial messages can be added to representations [41] or learned by the adversary [42]–[44]. However, these methods are inapplicable when victim agents do not communicate, a common assumption in many mainstream c-MARL algorithms [45]–[48].

C. RL Attacks by Adversarial Policy

Distinct from observation-based attacks, adversarial policy attacks do not necessitate access to victim observations or parameters (black-box). Rather, they introduce an adversarial agent whose actions are designed to deceive victim agents, causing them to take counterintuitive actions and ultimately fail to achieve their goals. In this paper, the terms "policy-based attack" and "adversarial policy" are used interchangeably. Gleave et al. [15] were the first to introduce adversarial policy in two-agent zero-sum games. Subsequent research has enhanced adversarial policy by exploiting victim agent vulnerabilities. Wu et al. [16] induced larger deviations in victim actions by perturbing the most sensitive feature in victim observations, identified through a saliency-based approach. However, larger deviations in victim actions do not necessarily correspond to strategically worse policies. Guo et al. [17] extended adversarial policies to general-sum games by simultaneously maximizing the adversary's reward and minimizing the victim's rewards. Yet, none of these studies have considered attacks in c-MARL settings.

D. Training c-MARL agents

Training c-MARL agents necessitates that multiple agents learn to cooperate effectively to achieve the highest joint reward. Early approaches, such as IQL [49], trained each agent individually. Subsequent methods aimed to address the credit assignment problem, with the objective of decomposing the joint value function to enable each agent's contribution to team success. Research in this area includes VDN [50], QMIX [45], COMA [47], QTRAN [51], QPLEX [52], and FACMAC [9]. Another line of research promotes cooperation by training decentralized agents using a centralized critic, as seen in MADDPG [48], IPPO [53], and MAPPO [46]. Alternative approaches foster cooperation by maximizing mutual information, or "influence", between agents. Such works include social influence [54], EITI/EDTI [55], VM3-AC [56], and PMIC [57]. In this paper, we train our c-MARL victims using MAPPO [46] as it performs well under both continuous and discrete control. After training, the victims' parameters are fixed during the attack.

III. Threat Model

In this section, we provide a detailed illustration of policy-based attack in c-MARL scenario.

A. Problem Definition

We conceptualize adversarial attacks targeting c-MARL agents within the framework of a partially observable Stochastic game (POSG) [58], which can be characterized by a tuple: $\langle\{N^\alpha, N^\nu\}, \mathcal{S}, \mathcal{O}, \{\mathcal{A}^\alpha, \mathcal{A}^\nu\}, \mathcal{T}, \{R^\alpha, R^\nu\}, \gamma\rangle$.

- The quantities N^α and N^ν represent the number of adversary agents and victim agents, respectively. Throughout this paper, we use α to designate the adversary and ν to indicate the victims. In scenarios where $N^\alpha = N^\nu = 1$, the problem simplifies to a two-agent adversarial policy, as previously examined in the literature [15]–[17].
- $\mathcal{S}$ represents the global environmental state. Adhering to the centralized training and decentralized execution (CTDE) paradigm in c-MARL [45]–[48], $\mathcal{S}$ is employed exclusively during training and not during testing (execution).
- $\mathcal{O} := O_1 \times ... \times O_{N^\nu + N^\alpha}$ denotes the local observations of both victim and adversarial agents. Each individual observation, $\mathcal{O}_i$, serves as an input for the policy networks of victims and adversaries.
- $\mathcal{A}^\nu := A_1^\nu \times ... \times A_{N^\nu}^\nu$ and $\mathcal{A}^\alpha := A_1^\alpha \times ... \times A_{N^\alpha}^\alpha$ represent the actions taken by victim and adversarial agents, respectively. Each agent selects their action using their own policy, with victims employing $\pi^\nu(a^\nu|o_i) : \mathcal{O} \mapsto \mathcal{A}^\nu$ and adversaries utilizing $\pi^\alpha(a^\alpha|o_i) : \mathcal{O} \mapsto \mathcal{A}^\alpha$, where o_i denotes the observation of each individual agent.
- $\mathcal{T} : \mathcal{S} \times \{\mathcal{A}^\alpha, \mathcal{A}^\nu\} \mapsto \mathcal{S}$ represents the environment transition function. Given the current state $s \in \mathcal{S}$ and joint action $\mathbf{a}^\nu \in \mathcal{A}^\nu$, $\mathbf{a}^\alpha \in \mathcal{A}^\alpha$ at the present timestep, $\mathcal{T}(s'|s, \mathbf{a}^\alpha, \mathbf{a}^\nu)$ computes the probability of transitioning to state $s' \in \mathcal{S}$ at the subsequent timestep.
- $\mathcal{R}^\nu, \mathcal{R}^\alpha : \mathcal{S} \times \{\mathcal{A}^\alpha, \mathcal{A}^\nu\} \times \mathcal{S} \mapsto \mathbb{R}$ signifies the reward function for both victims and adversaries after executing a joint action $\mathbf{a}^\nu \in \mathcal{A}^\nu$, $\mathbf{a}^\alpha \in \mathcal{A}^\alpha$ that transitions the state from $s \in \mathcal{S}$ to $s' \in \mathcal{S}$. A zero-sum game arises when $\mathcal{R}^\nu = -\mathcal{R}^\alpha$, whereas a general-sum game emerges in all other instances.
- γ represents the temporal discount factor employed in this study.

The objective of the attacker is to learn a policy, $\pi_\theta^\alpha(a^\alpha|o_i)$, parameterized by θ, that maximizes the expected discounted cumulative reward of the attacker, $J(\theta) = \mathbb{E}_{s,\mathbf{a}}[\sum_t \gamma^t r_t^\alpha]$, with $r_t^\alpha \in R^\alpha$. During the attack, the parameters of the victim policies remain fixed, which is a standard approach for stable deployment of reinforcement learning agents [59]. Consequently, the attacker must solve a reinforcement learning problem [15], but can exploit the weakness in policies of other agents by maximally deviating victims into a jointly worst-case situation. In this study, we assume the presence of a single attacker for simplicity (*i.e.*, $N^\alpha = 1$). To execute this adversarial attack, the attacker can influence the victim policies by taking adversarial actions $a^\alpha \in \mathcal{A}^\alpha$ learned by policy π^α at time t. These actions alter the observation $\mathcal{O}$ through environmental transitions, subsequently misleading the victim policies π^ν to produce suboptimal actions at time $t+1$.

B. Attacking Pathways and Applications

We propose two potential ways for attackers to initiate our AMI attack. The first and most pragmatic approach involves legally participating in a multi-agent distributed system [60], [61] and executing an adversarial policy as an individual agent. In applications such as autonomous driving [21]–[24],

distributed resource allocation [7], [18]–[20], and transmit power control [62], [63], an adversary can legitimately join the environment and take its own actions. Alternatively, an attacker can hijack an agent directly [64]–[66] and utilize the controlled agent to implement an adversarial policy. For instance, an adversary could compromise an unmanned aerial vehicle (UAV) within a UAV swarm and execute adversarial actions to fail other drones in applications such as surveillance [11] and delivery [67].

Aside from its malicious applications, our AMI attack also functions as a potent testing algorithm [68] for assessing the worst-case robustness of c-MARL algorithms. In real world, c-MARL agents may fail due to software/hardware error, or being compromised by an adversary. A strong attack algorithm such as AMI can better evaluate a more accurate worst-case performance of c-MARL agents. This assessment aids researchers in the development of robust algorithms and assists policy makers in managing algorithmic risks prior to deployment.

C. Adversary's Constraint and Capability

In this section, we elaborate on the constraints and capabilities of policy-based adversaries in c-MARL attacks. During an attack, the adversary possesses full control over the adversarial agent and can execute any physically feasible actions within its environment. The adversary acquires an adversarial policy by processing local observations as input and taking actions to influence victims at each timestep. Throughout the training phase, the adversarial policy is developed by engaging with victims in an iterative, trial-and-error process, typically within a simulated environment. In order to minimize the global team reward, the adversary assess to the state and adversary rewards only in training, which is accepted by other c-MARL adversarial attacks [12], [41], [43], [44].

In the context of black-box adversarial attacks against c-MARL agents, our attacker is more practical compared to previous white-box observation-based attacks [12]. Specifically, our attacker cannot directly manipulate agent observations but can only influence victims by interacting with the environment through its actions. Furthermore, our attacker cannot access other agents' models (e.g., architectures, weights, gradients). In contrast to the general-sum adversarial policy employed by *Guo et al.* [17], we assume that, due to the black-box constraint, the adversary cannot obtain victim rewards. Additionally, the adversary cannot choose which agent to control, nor can it switch from controlling its current agent to another agent across different timesteps.

Moreover, to deploy our AMI attack in a real world environment, we follow a Sim2Real paradigm [59] widely adopted in the reinforcement learning community. In this approach, the adversary trains its adversarial policy within a simulated environment initially, then freezes the policy's parameters and deploys the attack to real-world robots.

IV. Adversarial Minority Influence Approach

As previously mentioned, adversarial policy towards c-MARL presents two challenges: the *influence* challenge, which necessitates the adversary to maximize victim policy deviations under intricate agent-wise interactions; and the *cooperation* challenge, which requires the adversary to deceive agents into jointly worst failures. In this paper, we address these challenges through our *adversarial minority influence (AMI)* framework. As depicted in Fig. 2, AMI achieves potent attack capabilities by *unilaterally* guiding victims towards a *targeted* worst-case scenario. To maximize policy deviation of victims, we propose the *unilateral influence filter* that characterizes the adversarial impact from the adversary to victims by decomposing the bilateral mutual information metric and eliminating the detrimental influence from victims to the adversary. To steer victims towards jointly worst actions, the *targeted adversarial oracle* is a reinforcement learning agent that co-adapts with the adversary and generates cooperatively worst-case target actions for each victim at every timestep.

A. Unilateral Influence Filter

In a c-MARL attack, due to the intercorrelated nature of agent policies, targeting one victim inevitably impacts the policies of other victims as well. In light of such intricate relationships, maximizing policy deviations for victims necessitates that the adversary first characterizes the influence of its actions on each victim before maximizing that influence. Consequently, to delineate the unilateral influence from the adversary to the victim, we draw inspiration from the minority influence theory in social psychology [25], [69].

Using mutual information as a starting point, we emphasize that the policies of the adversary and the victims are interdependent. However, mutual information fails to fully reflect the deviation in victim policy as it includes the reverse influence - from the victims to the adversary - which is counterproductive for the attack. By focusing on this one-way influence, our approach aligns with the principles of minority influence, where a small, focused group can effect change within a larger group. This adds a nuanced, but critical, understanding of the dynamics at play in c-MARL attacks.

We begin by examining mutual information, a commonly employed bilateral influence metric in the c-MARL literature [54], [55], [57], [70], which captures the relationship between agents. For instance, considering social influence [54], the mutual information between the adversary action a_t^α and the influenced victim action $a_{t+1,i}^\nu$ can be expressed as $I(a_t^\alpha; a_{t+1,i}^\nu | s_t, \mathbf{a}_t^\nu)$, where a_t^α denotes the action taken by adversary α at time t, and $a_{t+1,i}^\nu$ represents the action taken by the i^{th} victim ν at time $t+1$. Practically, given the unknown nature of victim observation and parameters, the action probability of $a_{t+1,i}^\nu$ is approximated by a DNN parameterized by ϕ and trained via a standard supervised learning objective, i.e., $\max_\phi \sum_{i=1}^{N^\nu} \sum_{t=0}^{T-1} \log p_\phi(\hat{a}_{t+1,i}^\nu | s_t, \mathbf{a}_t)$, where T denotes the total timesteps of an episode. In the remainder of our paper, we use $\hat{a}$ to signify that the action is predicted, rather than ground truth.

Although mutual information is capable of characterizing agent-wise influence in c-MARL, it is important to note that *attacks towards c-MARL differ from cooperation due to the fixed nature of victim parameters*, which renders victim

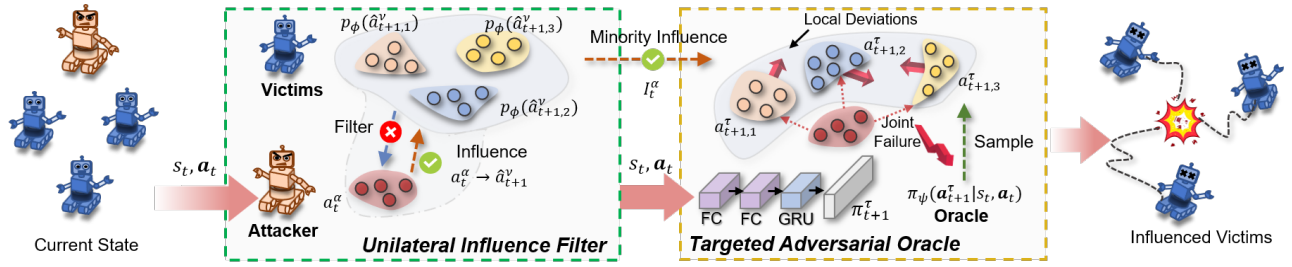

Fig. 2: The framework of AMI consists of two key components. The unilateral influence filter effectively decomposes mutual information into minority and majority influence terms while retaining the latter for asymmetric influence. Meanwhile, the targeted adversarial oracle is a reinforcement learning agent that generates the worst-case target for each victim. Directing victims toward this target culminates in the most unfavorable cooperative outcome.

actions more challenging to modify compared to those of the adversary. To demonstrate the effects of fixed victim policy, we decompose the mutual information between the adversary action a_t^α and a victim agent $a_{t+1,i}^\nu$ as follows:

$$I(a_t^\alpha; \hat{a}_{t+1,i}^\nu | s_t, \mathbf{a}_t^\nu) = \underbrace{-H(\hat{a}_{t+1,i}^\nu | s_t, a_t^\alpha, \mathbf{a}_t^\nu)}_{\text{majority}} + \underbrace{H(\hat{a}_{t+1,i}^\nu | s_t, \mathbf{a}_t^\nu)}_{\text{minority}}. \tag{3}$$

In the context of a c-MARL attack, we refer to the first term as *majority influence*, that is, the extent to which the minority (attacker) adapts its policy to conform with the policies of the majority (victims). In order to maximize mutual information, $H(\hat{a}_{t+1,i}^\nu | s_t, a_t^\alpha, \mathbf{a}_t^\nu)$ should be *minimized*, such that having knowledge of a_t^α reduces the uncertainty surrounding the victim policy. In policy-based attacks within c-MARL, the majority influence term in mutual information causes attackers to comply with victim policies, yielding high mutual information but weak attack capability. To elucidate this, consider that the parameters of victims are fixed, whereas the adversary policy is learned. We assume that it is significantly more straightforward to modify the adversary's policy than the victim's policy. Consequently, in order to minimize majority influence, the most effective approach for an attacker is to adjust its action a_t^α to render it more predictive of $a_{t+1,i}^\nu$, without actually altering $a_{t+1,i}^\nu$.

Simultaneously, the second term, $H(\hat{a}_{t+1,i}^\nu | s_t, \mathbf{a}_t^\nu)$, can be interpreted as a form of *minority influence* devoid of victim impact, reflecting solely the adversary's effect on victims. This term accounts for the entropy of the victim policy without conditioning on a_t^α, thereby establishing an *unilateral* metric. Given that the influence of the adversary action a_t^α is marginalized, the adversary is unable to modify its action to cater to the victims. *To further clarify the concepts of majority and minority influence, we have included a toy example in the supplementary materials, in which we meticulously demonstrate the two types of influence through experimentation.*

Building upon the aforementioned discourse, we examine and generalize minority influence within mutual information to enhance attack capabilities. In particular, maximizing minority influence necessitates that the current adversary policy exhibit substantial uncertainty in the victim policy. This can also be expressed as follows (*refer to supplementary material for derivation*):

$$\begin{aligned} H(\hat{a}_{t+1,i}^\nu | s_t, \mathbf{a}_t^\nu) &= -D_{KL}\left(p_\phi(\hat{a}_{t+1,i}^\nu | s_t, \mathbf{a}_t^\nu) || \ \mathcal{U}\right) + c \\ &= -D_{KL}\left(\mathbb{E}_{\tilde{a}_t^\alpha \sim \pi_t^\alpha}\left[p_\phi(\hat{a}_{t+1,i}^\nu | s_t, \tilde{a}_t^\alpha, \mathbf{a}_t^\nu)\right] || \ \mathcal{U}\right) + c, \end{aligned} \tag{4}$$

In the equation, $\mathcal{U}$ represents a uniform distribution for victim actions applicable to both discrete and continuous action spaces, while D_{KL} denotes the Kullback-Leibler divergence. Furthermore, c is a constant, and $\tilde{a}_t^\alpha$ refers to the counterfactual action sampled from the adversarial policy π_t^α.

Equation 4 indicates that the second term is equivalent to minimizing the KL divergence between the victim policy and the uniform distribution. For a more general relation metric between adversary and victim, we can release the constraints of Eqn. 4 and generalize $\mathcal{U}$ to any desired target distribution $\mathcal{D}$ and extend D_{KL} to any distance metric $d(\cdot, \cdot)$. Consequently, the unilateral influence can be expressed as:

$$I = d\left(\mathbb{E}_{\tilde{a}_t^\alpha \sim \pi_t^\alpha}\left[p_\phi(\hat{a}_{t+1,i}^\nu | s_t, \tilde{a}_t^\alpha, \mathbf{a}_t^\nu)\right], \ \mathcal{D}\right). \tag{5}$$

In this manner, influencing victims unilaterally is tantamount to minimizing the distance between the expected victim policy under the adversary policy and a target distribution.

B. Targeted Adversarial Oracle

Upon elucidating the maximization of victim policy deviations through unilateral influence, it remains crucial to ensure that victims are guided toward an optimal target. Merely deviating the victim policy arbitrarily or in the direction of a locally inferior case does not guarantee a globally worst-case failure for c-MARL. To enhance attack capability, it is necessary to ascertain globally worst target actions for victims and subsequently steer each victim toward its target $\mathcal{D}$ (Eqn. 5) using the proposed unilateral influence approach. Consequently, we introduce a reinforcement learning agent that learns these jointly worst target actions by co-adapting its policy with the attacker in a trial-and-error process.

To accomplish the targeted attack objective, we introduce the *Targeted Adversarial Oracle (TAO)*, a reinforcement learning agent π_ψ parameterized by ψ, which guides the attacker in unilaterally influencing each victim toward a targeted local policy. When all victims are influenced in this manner, they collectively form a worst-case scenario for cooperative agents. We denote the action and policy used by TAO as τ. As an RL

agent, TAO adjusts to the current perturbation budget of the adversary through a trial-and-error process: if the adversary can significantly impact victim policies, TAO can generate the target more aggressively, directing victims to undertake riskier actions, thus achieving greater attack capability; conversely, if the adversary has limited influence on victims, TAO strives to introduce minor yet effective perturbations to victims, which is feasible under the current perturbation budget.

Analogous to the attacker, TAO's objective is to maximize the adversary's goal. Consequently, we train TAO's policy to optimize the accumulated adversarial reward r^α utilizing proximal policy optimization (PPO) [71]:

$$\begin{aligned} &\max_{\psi} \mathbb{E}_{\pi^\tau_\psi} \left[\min\left(\text{clip}\left(\rho_t, 1-\epsilon, 1+\epsilon\right) A^\tau_t, \rho_t A^\tau_t\right)\right], \\ &\text{where} \quad \rho_t = \frac{1}{N^\nu} \sum_{i=1}^{N^\nu} \frac{\pi^\tau_\psi(a^\tau_{t+1,i}|s_t, \mathbf{a}^\nu_t, a^\alpha_t)}{\pi^\tau_{\psi_{old}}(a^\tau_{t+1,i}|s_t, \mathbf{a}^\nu_t, a^\alpha_t)}, \end{aligned} \tag{6}$$

In this context, $\pi^\tau_{\psi_{old}}$ and π^τ_ψ represent the previous and updated policies for TAO, respectively. A^τ_t refers to the advantage function determined by the generalized advantage estimation (GAE) [72]. The function $clip(\rho_t, 1-\epsilon, 1+\epsilon)$ constrains the input ρ_t within the limits of $1-\epsilon$ and $1+\epsilon$.

In this case, the policy $\pi^\tau_{\psi,i}(\cdot|s_t, \mathbf{a}t)$, as determined by TAO, functions as the desired target distribution $\mathcal{D}$ in Eqn. 5 for victim i at time t. Notably, as PPO is an on-policy algorithm, actual actions must be executed at each timestep. Consequently, $\mathcal{D}$ is derived by sampling a target action $a^\tau_{t+1,i}$ from $\pi^\tau_{\psi,i}$ instead.

C. Overall Training

In summary, the influence metric I^α_t employed by AMI at time t incorporates the optimal target action $a^\tau_{t+1,i}$, generated by TAO, as the target distribution $\mathcal{D}$ in the unilateral influence found in Eqn. 5:

$$\begin{aligned} I^\alpha_t = \sum_{i=1}^{N^\nu} \Bigg[& d\Big(\mathbb{E}_{\tilde{a^\alpha_t} \sim \pi^\alpha_t}\Big[p_\phi(\hat{a}^\nu_{t+1,i}|s_t, \tilde{a}^\alpha_t, \mathbf{a}^\nu_t)\Big], \\ & a^\tau_{t+1,i} \sim \pi^\tau_\psi(\cdot|s_t, a^\alpha_t, \mathbf{a}^\nu_t)\Big)\Bigg], \end{aligned} \tag{7}$$

In the case of $d(\cdot,\cdot)$ as the distance function for AMI, the calculation differs depending on the control setting. For *discrete control*, the distance function is computed as $d(p(\hat{a}^\nu_i|s, \mathbf{a}), a^\tau_i) = -||p(\hat{a}^\nu_i|s, \mathbf{a}) - \mathbf{1}_\mathcal{A}(a^\tau_i)||_1$, where $p(\hat{a}^\nu_i|s, \mathbf{a})$ is a shorthand for $\mathbb{E}_{\tilde{a^\alpha_t} \sim \pi^\alpha_t}\left[p(\hat{a}^\nu_{t+1,i}|s_t, \tilde{a}^\alpha_t, \mathbf{a}^\nu_t)\right]$ and a^τ_i denotes $a^\tau_{t+1,i}$. $\mathbf{1}_\mathcal{A}(a^\tau_i) = [a^\tau_i \in \mathcal{A}^\tau_i]$ is the indicator function with action space $\mathcal{A}^\tau_i$. A negative sign is added to minimize the distance between the one-hot target action $\mathbf{1}_\mathcal{A}(a^\tau_i)$ and the victim action probability. In the case of *continuous control*, the distance function is calculated as $d(p(\hat{a}^\nu_i|s, \mathbf{a}), a^\tau_i) = p(a^\tau_i|s, \mathbf{a})$, such that the target action $a^\tau_{t+1,i}$ has a high probability in the estimated victim action probability distribution. Empirically, we find that our method is not sensitive to the choice of distance functions.

In the final step, I^α_t serves as an auxiliary reward that is optimized by the policy of the adversarial agent $\pi_\theta(a^\alpha_t|o^\alpha_t)$, parameterized by θ. The reward r^{AMI}_t for the adversarial agent π_θ to optimize can be expressed as:

$$r^{AMI}_t = r^\alpha_t + \lambda \cdot I^\alpha_t, \tag{8}$$

In this case, λ represents a hyperparameter that balances the trade-off between the adversary reward r^α_t and maximizing the influence I^α_t on the victim agents. Once more, we compute the advantage function A^α_t using r^{AMI}_t via Generalized Advantage Estimation (GAE) [72], and train the adversary policy π_θ employing Proximal Policy Optimization (PPO) [71]:

$$\begin{aligned} &\max_{\theta} \mathbb{E}_{\pi^\alpha_\theta} \left[\min\left(\text{clip}\left(\rho_t, 1-\epsilon, 1+\epsilon\right) A^\alpha_t, \rho_t A^\alpha_t\right)\right], \\ &\text{where} \quad \rho_t = \frac{\pi^\alpha_\theta(a^\alpha_t|o^\alpha_t)}{\pi^\alpha_{\theta_{old}}(a^\alpha_t|o^\alpha_t)}. \end{aligned} \tag{9}$$

The complete training procedure is outlined in Algorithm 1. In particular, we initially roll out K trajectories, obtaining s_t and $\mathbf{a}t$ utilizing the current policies of the attacker and victims. Subsequently, we train the opponent modeling module $p_\phi(\hat{a}^\nu_{t+1,i}|s_t, \mathbf{a}_t)$ and update the targeted adversarial oracle's actor $\pi_\psi(\cdot|s_t, \mathbf{a}_t)$ and critic A^τ_t. Ultimately, we compute the reward r^{AMI}_t using Equation 8 and update the attacker's actor $\pi^\alpha_\theta(\cdot|o^\alpha_t)$ and critic A^α_t.

Algorithm 1 Adversarial Minority Influence Algorithm.

Input: Policy network of victim agents π^ν, policy network of adversary agent π_θ, value function network of adversary agent V^α, network of opponent modelling p_ϕ, policy network of targeted adversarial oracle (TAO) π_ψ, value function network V^τ of TAO.

Output: Trained policy network of adversary agent π_θ.

1: **for** k = 0, 1, 2, ... K **do**
2: Perform rollout using current adversarial policy network π_θ and TAO agent π^τ_ψ. Collect a set of trajetories $\mathcal{D}_k = \tau_i$, where i = 1, 2, ..., $|\mathcal{D}_k|$.
3: Update opponent modelling model p_ϕ.
4: Calculate advantage function of TAO A^τ_t by GAE, using value function V^α and adversary reward r^α; Update value function network V^τ of TAO.
5: Update the policy network π_ψ of TAO using Eqn. 6;
6: Calculate reward r^{AMI}_t for adversary by Eqn. 8.
7: Calculate advantage function A^α_t by GAE, using value function V^α and reward r^{AMI}; Update value function network V^α of adversary.
8: Update policy network π_θ of adversary by Eqn. 9.
9: **end for**

V. Experiments

In this section, we perform comprehensive experiments in both simulated and real-world environments to assess the effectiveness of our AMI approach in terms of attack capability.

A. Experimental Setup

1) Environments and implementation details: We assess the effectiveness of AMI in three distinct environments: (1) A real-world multi-robot rendezvous environment, in which

robot swarms learn to congregate, known as *rendezvous* [10]. (2) StarCraft Multi-Agent Challenge (SMAC) [5], involving discrete control across six tasks, where the objective is to control a group of agents in a StarCraft game to defeat an opposing group; (3) Multi-Agent Mujoco (MAMujoco) [9] for continuous control, comprising six tasks that require controlling robotic joints to optimize speed in a specific direction. All victim policies were trained using MAPPO [46]. During the attack, the first agent is selected as the adversary, unless otherwise specified. *Additional implementation details can be found in the supplementary materials.*

2) Compared methods and evaluation metrics: We benchmark AMI against state-of-the-art adversarial policy methods, including *Gleave et al.* [15], *Wu et al.* [16], and *Guo et al.* [17]. While these methods were initially designed to target single-agent RL, we adapt them to attack c-MARL by substituting a single RL victim with multiple RL victims. To ensure a fair comparison, AMI and all baselines employ the same codebase, network structure, and hyperparameters. For method-specific hyperparameters, we tune their values for optimal performance.

The adversary's goal is to maximize the adversarial reward r^{α}, which is adapted from the victim reward by (1) incorporating the loss of allies in addition to the loss of enemies (SMAC). The goal of the attacker is to fool its allies, not the enemies. (2) eliminating auxiliary reward terms in MAMujoco and rendezvous, such as penalty of victims taking actions of large magnitude, which is unrelated to the objective of the adversary. *A detailed description of the adversary reward can be found in the supplementary materials*. In this manner, akin to *Guo et al.*, the adversary and victims form a general-sum game, although we do not assume assess to victim rewards. We discover that using our adversary reward enhances overall attack capability in the discussion. Consequently, we train AMI and all baselines utilizing our adversary reward r^{α}, and employ the same reward as our evaluation metric (a higher value signifies stronger attack capability). All experiments were conducted with five random seeds, and results are presented with a 95% confidence interval. *Due to space constraints, detailed baseline implementations and hyperparameters are provided in the supplementary material.*

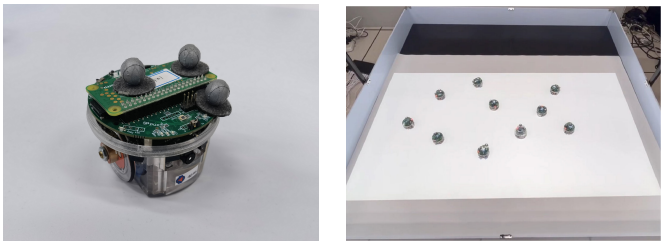

(a) E-puck2 robot (b) Playground

Fig. 3: Illustration of the robot and playground for our real-world multi-robot rendezvous environment. *See videos in our github repository.*

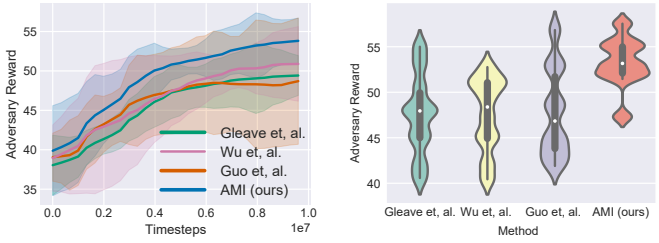

(a) Simulation (b) Real World

Fig. 4: Comparisons of AMI against baselines in simulation and real-world experiments.

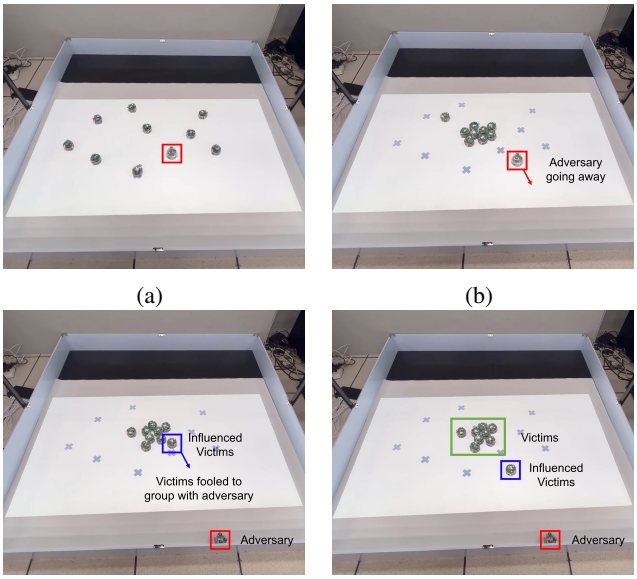

(a) (b) (c) (d)

Fig. 5: Behaviors of robot swarms under our AMI attack, adversary indicated by red square. Our adversary is the only one to fool away an agent to group with our adversary.

B. AMI Attack in Real World

To highlight the effectiveness of AMI, we evaluate AMI in real-world multi-robot environments. To the best of our knowledge, this marks the first demonstration of adversarial policy in real-world. As shown in Fig. 3, we create an environment with 10 e-puck2 robots (Fig. 3a) [73] in an indoor playground (Fig. 3b). The task is called *rendezvous*, where robots are randomly dispersed in the arena and must gather together. To mitigate the impact of randomness in initialization of robot positions, we employ a within-subject experimental design, ensuring that for all compared methods, the e-puck2 robots start from the same position within each run.

We train these robots using the widely adopted Sim2Real paradigm [59] in the RL community, in which agents first learn their policy in a simulated environment before being deployed in the real world with fixed parameters. To evaluate attack performance, we present results from both simulated and real-world scenarios in Fig. 4. Each method was tested 10 times in the real world, leading to several key findings:

(1) AMI outperforms all baselines in both simulated and real-world environments. The improvement of AMI in the real world is statistically significant ($p < .05$) compared to all baselines under a paired samples t-test and, on average, 5.43 higher than the best-performing baseline in the real world.

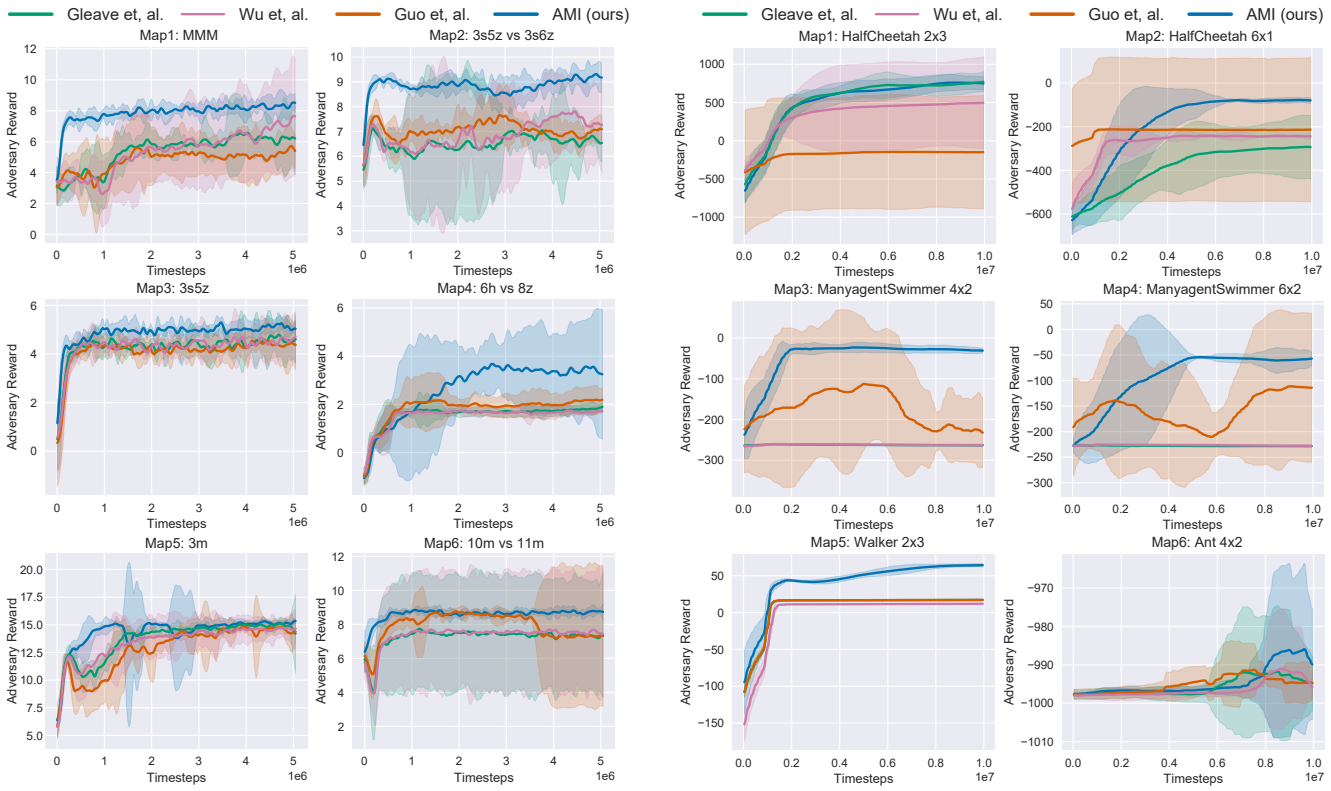

(a) SMAC Environment

(b) MAMujoco Environment

Fig. 7: Learning curves for AMI and baseline attack methods in (a) six SMAC and (b) six MAMujoco environments. The solid curves correspond to the mean, and the shaped region represents the 95% confidence interval over 5 random seeds.

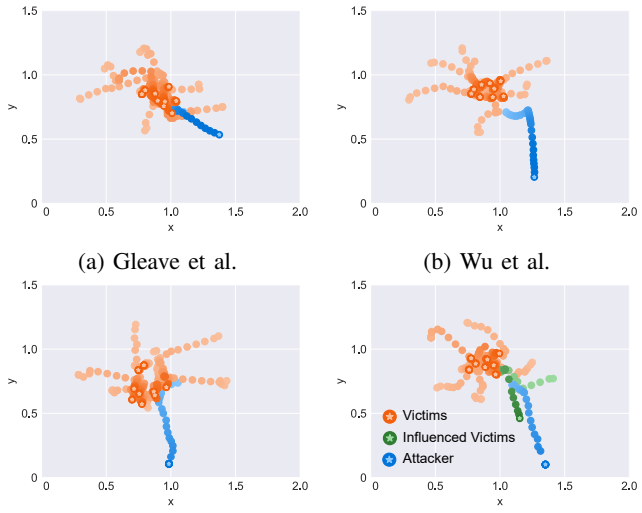

(a) Gleave et al.

(b) Wu et al.

(c) Guo et al.

(d) AMI (ours)

Fig. 6: Comparison of the trajectories of AMI and other baselines. AMI is the only method that could fool a victim away from the gathered victims (green dots). Lighter points indicate early timesteps and darker points indicate latter timesteps. Points with a star denote the final position.

(2) The superiority of AMI can be further demonstrated by agent trajectories and videos. As shown in the final state photographed in Fig. 5, victims first gather together as usual, with adversaries moving away (Fig. 5a, 5b). However, after that, one victim gets influenced by the adversary, and are fooled to gather with the adversary, instead of majority victims (Fig. 5c, 5d). As shown in the trajectories in Fig. 6, AMI is the only method to achieve this, with lighter points representing early timesteps and darker points indicating later timesteps. *Videos of these experiments can be found in our GitHub repository.*

C. AMI Attack in Simulation Environment

In this section, we conduct an empirical assessment of AMI's effectiveness in simulated environments. We compare AMI with baseline methods across six discrete control tasks (SMAC) and six continuous control tasks (MAMujoco), demonstrating its superior performance. For simplicity, we assume the attacker controls the first agent in all environments. The results depicted in Fig. 7 lead to several key observations:

(1) By strategically influencing victims toward a jointly worst target, AMI outperforms the competing methods in 10 out of 12 environments across both continuous and discrete control, thereby highlighting the effectiveness of our approach.

(2) Our experimental results suggest that the dimensionality controlled by the adversary is not the sole factor determining victim vulnerability in c-MARL, offering a complementary perspective to the claims made by *Gleave et al*. For instance, AMI demonstrates superior attack capability in the *Swimmer 4x2* environment, while all attacks are ineffective in *Ant 4x2*, despite the same dimensionality. We hypothesize that certain tasks may be intrinsically robust due to factors such as stable environment dynamics (*i.e.*, the environment provides similar

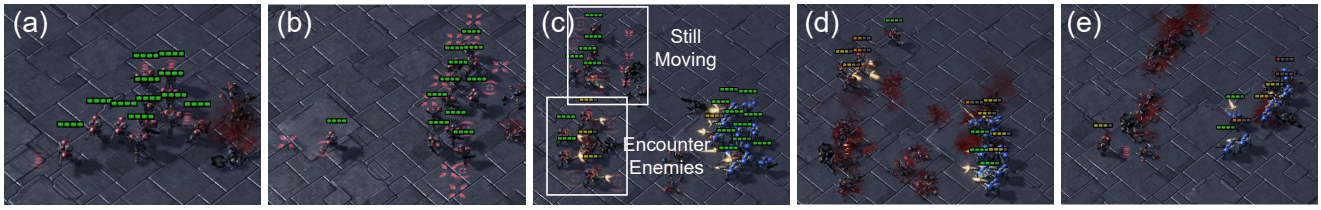

Fig. 7: Understanding the behavior of AMI. Attacker and victims in red, enemies in blue. (a) attackers entice victims to get back. (b) victims were influenced into a bad position. (c) some victims encounter enemies, while others are still moving. (d) first-arrived victims died, and enemies focused fire on the rest. (e) attacker moves near to get killed.

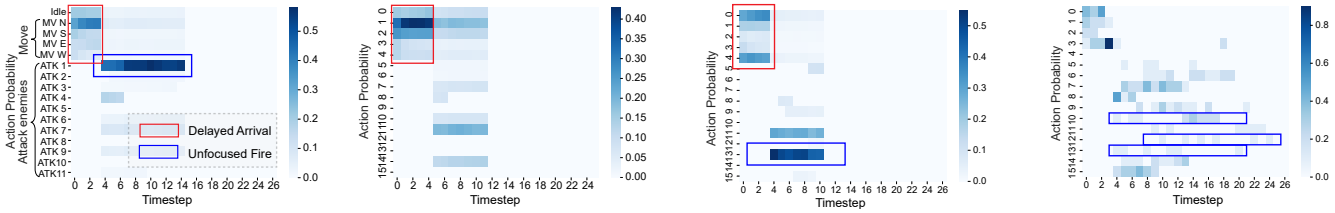

(a) TAO, Agent 3 (High AMI) (b) TAO, Agent 7 (Low AMI) (c) TAO, Agent 9 (High AMI) (d) Joint Victim Actions

Fig. 8: Actions suggested by TAO and taken by victims, evaluated in *10m vs 11m*. Red and blue bracket indicates delayed arrival and unfocused fire behavior of AMI. MV N means move north and ATK X means attack enemy ID X.

observations under various adversary actions), limited attacker capability (*i.e.*, the attacker controls an inconsequential agent), or weak cooperation between the attacker and victims (*i.e.*, agents do not cooperate and do not condition their policy on the adversary's actions).

(3) In environments like *3m*, all baselines converge to the same point with low variance. This suggests some environments possess simple dynamics and can be easily attacked, enabling all attacks to readily converge to the optimal policy.

(4) The method proposed by *Guo et al.* exhibits high variance in several MAMujoco environments. We discovered that this variance is associated with the general sum setting (using victim reward) and their method (training the adversary using two critics). *Further discussions regarding these findings can be found in the supplementary materials.*

In addition to assigning the adversary to control the first agent, we also investigate the attack capability of AMI when the adversary controls agents with different IDs, each possessing distinct initializations and functionalities. Results from experiments in which the adversary attacks through all possible agent IDs in the *3s5z vs 3s6z* environment demonstrate that the superiority of AMI remains consistent across different adversary IDs. *Detailed results can be found in the supplementary materials.*

D. Analyzation of AMI policies

To investigate the attack strategy of AMI, we visualize the behavior of victims subjected to AMI attacks in *10m vs 11m* environment of SMAC, shown in Fig. 7 and 8. *As for MAMujoco environment, we find while baseline attacks physically interfere with victims, they are still able to move in +x direction to get reward. In contrast, AMI fools victims towards jointly worst policy by fooling it to move clockwise. See details in Supplementary Materials.* We observe the following key findings for SMAC:

Victim behavior under AMI. Victims under AMI attack exhibit two critical behaviors that contributes to collective failure: (1) *delayed arrival*. As depicted in Fig. 7, victims are influenced by the attacker and divided into two groups. These groups encounter enemies at different timesteps: while some victims confront the full force of their adversaries, others are still approaching and do not have enemies within their firing range. (2) *unfocused fire*. In SMAC, focused fire involves allies collaboratively attacking and defeating enemies one at a time. However, in the presence of the attacker, allies fire in an *unfocused* manner. As illustrated in Fig. 8d, victims' shots at enemies (Action ID 5-15) are randomly distributed, lacking a coordinated target. Consequently, victims fail to eliminate enemy units and face stronger enemy fire.

Influence through the lens of TAO. The behavior of victims under AMI can be explained by the target actions generated by TAO. As demonstrated in Fig. 8, for understanding *delayed arrival*, at the game's onset, victims 3 and 7 are encouraged to move north (Action ID 1), arriving later compared to agents moving directly east; for victim 9, which is moving east, it is encouraged to move west or stay idle: had it followed this target, it would have arrived slightly later than agents moving east directly (*i.e.*, not being influenced), but still earlier than agents moving north, also resulting in delayed arrival. To comprehend *unfocused fire*, agents 3, 7, and 9 are encouraged to attack *different* enemies at the current timestep, limiting the number of victims attacking each enemy and suppressing focused fire.

Adaptive target generation. Furthermore, we discover that TAO can generate adaptive policies for victims with varying susceptibility, as illustrated in Fig. 8. By calculating AMI, we find that agents 3 and 9 are more influenced, and their target policies learned by TAO are more deterministic. In this manner, TAO generates a *targeted* goal for susceptible agents, as they have a higher probability of being influenced toward the collectively worst target policy. Conversely, since

agent 7 is less influenced, the target policy learned by TAO is less deterministic. In this case, TAO generates an *untargeted* goal for insusceptible agents: as their policies are difficult to influence, the attacker achieves the best results by preventing them from playing the optimal policy at the current timestep. In this way, TAO automatically learns different policies for susceptible and insusceptible victims under the current attacks.

E. Ablations

In this section, we verify the effectiveness of each component in our model. We conduct all experiments on *3s5z vs 3s6z* for SMAC and *HalfCheetah 6x1* for MAMujoco.

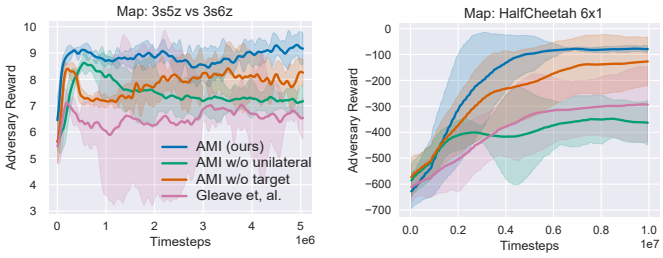

(a) SMAC environment (b) MAMujoco environment

Fig. 9: Ablation of unilateral and targeted properties of AMI. Both properties improve attack performance.

1) Ablations on unilateral and targeted properties: In this ablation study, we seek to assess the individual contributions of AMI's unilateral and targeted attack properties. For a version of AMI without unilateral attack capabilities, we integrate the majority influence term from Eqn. 3 into Eqn. 7, resulting in bilateral influence. In contrast, for AMI without a targeted attack, we employ Eqn. 4 as the influence metric. We also provide a comparison with the results of *Gleave et al.* (*i.e.*, absent of unilateral and targeted attacks). As illustrated in Fig. 9, the effectiveness of AMI relies on both enhancements. Notably, we observe that AMI without unilateral attack capabilities underperforms *Gleave et al.* in the *HalfCheetah 6x1* environment. This finding implies that majority influence can strongly diminish attack capability by encouraging the attacker to modify its actions to overfit to victim policies.

TABLE I: In this section, we address the distance metrics employed for both discrete and continuous environments. AMI is determined using these metrics and subsequently maximized by the attacker under the optimal hyperparameter λ.

Name	Equation	Environment
ℓ_1	$-\|\|p(\hat{a}_i^\nu\|s,\mathbf{a}) - \mathbf{1}_{\mathcal{A}}(a_i^\tau)\|\|_1$	Discrete
ℓ_2	$-\|\|p(\hat{a}_i^\nu\|s,\mathbf{a}) - \mathbf{1}_{\mathcal{A}}(a_i^\tau)\|\|_2$	Discrete
ℓ_∞	$-\|\|p(\hat{a}_i^\nu\|s,\mathbf{a}) - \mathbf{1}_{\mathcal{A}}(a_i^\tau)\|\|_\infty$	Discrete
CE	$\log(p(a_i^\tau\|s,\mathbf{a}))$	Discrete
Prob	$p(a_i^\tau\|s,\mathbf{a})$	Discrete
ℓ_1	$-\|\|\hat{\mu}_i^\nu(s,\mathbf{a}) - a_i^\tau\|\|_1$	Continuous
CE	$\log(p(a_i^\tau\|s,\mathbf{a}))$	Continuous
Prob	$p(a_i^\tau\|s,\mathbf{a})$	Continuous

2) Ablations on distance metric: Next, we investigate the performance of AMI when utilizing various distance metrics. We present alternative distance metrics for both discrete and continuous environments in Table I, where $\hat{\mu}_i^\nu(s,\mathbf{a})$ represents the mean predicted by the opponent modeling for continuous control, under the assumption that actions adhere to a Gaussian distribution. The outcomes are illustrated in Fig. 10, which reveals that the attack capability of AMI remains largely unaffected by the choice of distance metrics for both continuous and discrete control scenarios. Notably, the metrics employed in our AMI (ℓ_1 for discrete control and Prob for continuous control) yield the most favorable results.

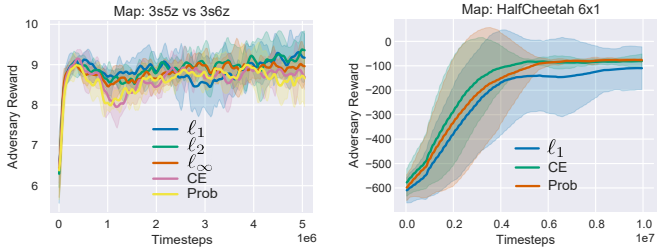

(a) Distance - Discrete (b) Distance - Continuous

Fig. 10: Ablation on distance metric. The performance of AMI is stable under different distance metrics.

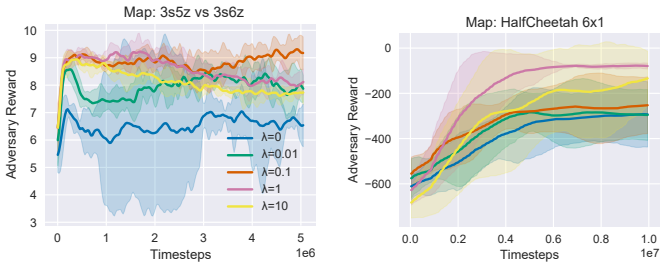

(a) SMAC environment (b) MAMujoco environment

Fig. 11: Ablation on hyperparameter λ. $\lambda = 0$ reduce to the method of *Gleave et al*. AMI achieves better results than baseline under different λ.

3) Ablations on hyperparameter: Lastly, we examine the performance of AMI under varying hyperparameters λ, which modulate the contribution of the AMI reward I_t^α to the total reward. Specifically, we assess our AMI attack for $\lambda = \{0, 0.01, 0.1, 1, 10\}$, where $\lambda = 0$ reverts to the method of *Gleave et al*. As depicted in Fig. 11, incorporating AMI enhances the overall attack performance compared to *Gleave et al*, thereby demonstrating the effectiveness of our approach. Moreover, selecting an appropriate hyperparameter leads to optimal AMI performance ($\lambda = 0.1$ in *3s5z vs 3s6z* and $\lambda = 1$ in *HalfCheetah 6x1*). We also observe that performance does not improve monotonically with increasing λ values. This can be attributed to the following factors: (1) a large λ generates high rewards, which may introduce instability when training the critic network, and (2) a substantial λ causes errors in the opponent modeling module p_ϕ to accumulate, resulting in excessive emphasis on the attack capability of the subsequent timestep.

F. Discussions

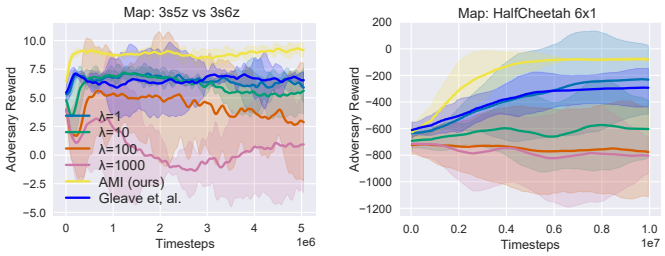

(a) SMAC environment (b) MAMujoco environment

Fig. 12: Using mutual information proposed in [54] as influence metric. Since mutual information is bidirectional, such metric was ineffective for attack.

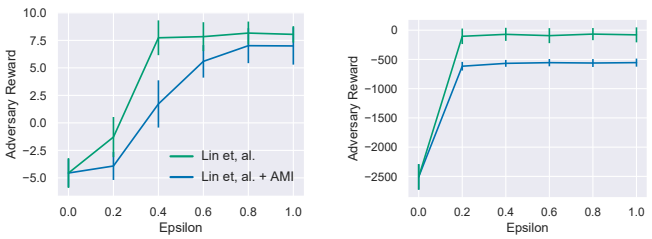

(a) SMAC environment (b) MAMujoco environment

Fig. 14: Using AMI as adversarial policy for state-based c-MARL adversary. AMI improves the power of state-based adversary by learning a more harmful policy under multiple perturbation budgets ϵ. $\epsilon = 0$ refers to no attack.

1) Comparing with mutual information: We begin by examining the attack capability of mutual information as an influence metric, which can be considered a bilateral and untargeted version of AMI. We implement mutual information based on the work of [54] and evaluate the results for four different λ values that modulate the magnitude of mutual information. As illustrated in Fig. 12, utilizing mutual information often results in inferior performance compared to *Gleave et al.* (*i.e.*, not employing mutual information). Moreover, the outcome worsens as λ increases. These observations serve as motivation for the development of AMI, a unilateral and targeted influence designed for c-MARL attacks, which yields superior performance.

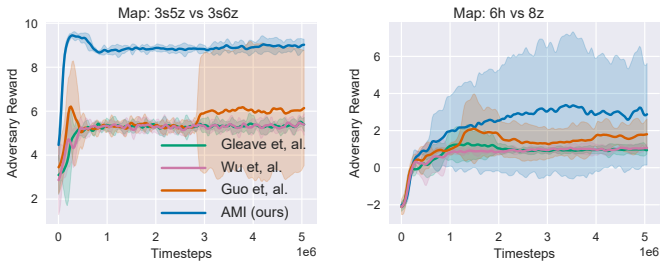

(a) QMIX, 3s5z vs 3s6z (b) QMIX, 6h vs 8z

Fig. 13: Attacking QMIX by AMI. The superior result of AMI is consistent in MAPPO and QMIX. MAMujoco is not evaluated since QMIX does not support continuous control.

2) Attacking other c-MARL algorithms: We have previously demonstrated that AMI attains superior results in attacking MAPPO victims, a representative actor-critic based method in c-MARL. We further illustrate that AMI is equally applicable to Q-learning based methods, such as QMIX [45]. As depicted in Fig. 13, our AMI consistently outperforms baseline adversarial policy methods in the *3s5z vs 3s6z* and *6h vs 8z* environments. We restrict our experiments to the SMAC environment, as Q-learning based methods are not designed to support continuous control.

3) Aiding state-based c-MARL adversary with AMI: AMI demonstrates superior results compared to baseline policy-based attacks. However, since observation-based attacks in c-MARL [12] employ adversarial policies to aid their attacks, we can enhance the performance of these attacks by utilizing AMI as a more potent adversarial policy. Following the approach outlined by *Lin et al.* [12], we replace the *stage 1* attack of *Lin et al.* from the c-MARL extension of *Gleave et al.* with our AMI attack, while maintaining the *stage 2* attack unchanged (i.e., generating observation perturbation using the same gradient-based method). The ℓ_∞ perturbation budget ϵ for observations is set to $\{0, 0.2, 0.4, 0.6, 0.8, 1\}$. Note that $\epsilon = 0$ signifies no attack. The results are presented in Fig. 14. As observation-based attacks also depend on adversarial policies to deceive victims into targeted actions, AMI can be directly employed to achieve improved attack performance in observation-based attacks, illustrating the generality of our proposed AMI as an adversarial policy.

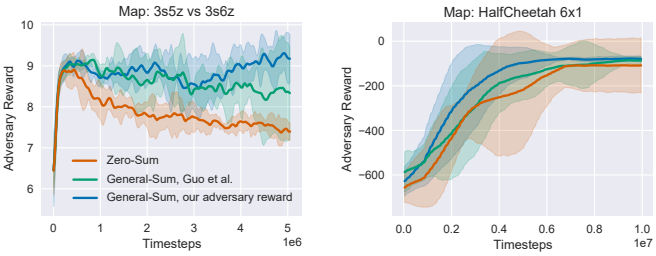

(a) SMAC environment (b) MAMujoco environment

Fig. 15: Attack capability of using reward setting of zero-sum, general-sum proposed by *Guo et al.* and our general-sum adversarial reward. Our general-sum reward achieves the best attack capability.

4) Using adversary reward for AMI: In earlier adversarial policy research by *Gleave et al.* and *Wu et al.*, the assumption is that the adversary's reward is the negative of the victim's reward, creating a *zero-sum* game between the adversary and victims. *Guo et al.* propose that the adversary possesses its own objective, establishing a *general-sum* setting and achieving stronger attack capabilities by jointly minimizing victim reward and maximizing adversary reward. However, in practice, obtaining victim rewards in general-sum games can be challenging for the adversary due to the black-box assumption. Therefore, our AMI maintains the general-sum setting but assumes access only to adversary reward, which can be freely defined and calculated from observation. We empirically assess the attack capabilities of these three reward types. As shown in Fig. 15, modeling adversarial attacks as a general-sum game results in higher attack capabilities (SMAC)

and improved convergence during training (MAMujoco) compared to a zero-sum setting. Furthermore, in general-sum games, our adversary reward outperforms the objective utilized by *Guo et al.*, indicating that minimizing victim reward is not essential for a potent general-sum attack. Consequently, since our general-sum adversarial reward yields superior attack capabilities overall, we use this reward to train our AMI attack and all baselines for a fair comparison.

VI. Countermeasures Against AMI

In this section, we introduce two potential defensive strategies against our AMI approach and assess their effectiveness, namely adversarial training and adversarial detection. Specifically, adversarial training involves retraining victim agents to optimize their performance in the presence and absence of an adversary, while adversarial detection employs a binary classifier to determine the existence of an adversary at each timestep. We continue to use the *3s5z vs 3s6z* scenario for the SMAC environment and the *HalfCheetah6x1* setup for the MAMujoco environment as our testbed.

A. Adversarial Training

Adversarial training (AT) is a general strategy employed to enhance the robustness of reinforcement learning by training the victim policy to maximize rewards in the presence of an adversary. In the context of c-MARL, we adopt the *dual training* approach utilized by [15], [17]. In this method, during each episode (*i.e.*, one round of the game), victims are trained to play with the 1^{st} agent, which can either be an AMI adversary with fixed policy network parameters or a benign policy executed by the current victims. This approach ensures that the victims perform well both with and without an attack, rather than only defending against adversaries but failing in their absence.

Although adversarial training provides a promising defense against a fixed AMI adversary, we further investigate whether such defenses can be overcome by new adversaries. We propose two countermeasures against adversarially trained victims: (1) *re-AMI*, which evaluates if adversarially trained victims can be re-attacked by a newly trained adversary. Following [15], we retrain a new AMI adversary in the same position (*i.e.*, 1^{st} agent) against adversarially trained victims. (2) *pos-AMI*, which evaluates if adversarially trained victims against one position (*e.g.*, 1^{st} agent) remain resilient against adversaries in different positions (*e.g.*, adversary controlling 2^{nd} agent). This threat is unique to the c-MARL setting.

For better comparison, we present a summary of the results for two types of victims (*i.e.*, normally trained victims and adversarially trained victims) against four types of adversaries (*i.e.*, no adversaries, AMI, re-AMI, and Pos-AMI) in Table. II. Several conclusions can be drawn from these results:

(1) Adversarial training serves as a general defense approach, effectively defending against our AMI attack when the defender is aware of the adversary's policy and position (-3.16 adversarial reward for *3s5z vs 3s6z* and -1384.05 for *HalfCheetah 6x1*). Moreover, such defense does not significantly degrade normal performance in the absence of an attack

TABLE II: Adversarial training (AT) results on SMAC and MAMujoco, adversarial reward reported with mean and standard deviation (lower means higher robustness).

Adversary	Victims	3s5z vs 3s6z	HalfCheetah 6x1
None	Normal	$-4.399_{\pm 3.917}$	$\mathbf{-2310.18}_{\pm 666.81}$
	AT	$\mathbf{-4.928}_{\pm 3.779}$	$-2040.29_{\pm 75.22}$
AMI	Normal	$9.008_{\pm 2.900}$	$-72.57_{\pm 54.81}$
	AT	$\mathbf{5.843}_{\pm 4.612}$	$\mathbf{-1456.62}_{\pm 48.18}$
Re-AMI	Normal	$7.996_{\pm 4.015}$	$\mathbf{-620.14}_{\pm 20.04}$
	AT	$\mathbf{5.111}_{\pm 5.365}$	$-18.40_{\pm 16.76}$
Pos-AMI	Normal	$10.366_{\pm 1.774}$	$-352.11_{\pm 84.61}$
	AT	$\mathbf{8.231}_{\pm 3.624}$	$\mathbf{-1237.92}_{\pm 68.82}$

(-0.529 for *3s5z vs 3s6z* and +269.89 for *HalfCheetah 6x1*). In fact, adversarial training slightly improves normal performance in the *3s5z vs 3s6z* scenario.

(2) While adversarially trained victims demonstrate robustness to *re-AMI* in *3s5z vs 3s6z*, they are not robust in *HalfCheetah 6x1*, indicating the possibility of adversarially trained agents being re-attacked. We hypothesize that this non-robustness stems from the varying number of vulnerabilities in c-MARL policies: in *3s5z vs 3s6z*, victim policies may have a limited number of weaknesses that can be addressed through adversarial training, making re-trained AMI unable to exploit additional vulnerabilities. However, in *HalfCheetah 6x1*, victim policies may possess numerous intrinsic weaknesses. Since adversarial training might not rectify all vulnerabilities, re-trained AMI can still attack the policy by exploiting other weaknesses. To further improve robustness against *re-AMI*, we propose iteratively refining the adversarial training process using re-trained AMI policy and training new AMI policy against the updated victims.

(3) Additionally, we observe that adversarial training somewhat enhances robustness against *pos-AMI* (-2.135 in *3s5z vs 3s6z* and -885.81 in *HalfCheetah 6x1*), but remains less robust compared to adversarially trained AMI policy (+2.39 in *3s5z vs 3s6z* and +218.7 in *HalfCheetah 6x1*). This result can be interpreted as follows: first, some weaknesses in victim policies are *position-agnostic*. For instance, AMI in different positions can influence victims to adopt similar suboptimal actions. Addressing such position-agnostic weaknesses generalizes the defensive capability of adversarial training towards the 1^{st} adversary to other positions. Second, since *pos-AMI* adversaries possess distinct initialization and functionality, they can maximize their attack capability by probing *position-specific* vulnerabilities in victim policies. Therefore, constructing robust c-MARL policy against policy-based attacks requires considering both *position-agnostic* and *position-specific* vulnerabilities.

B. Adversarial Detection

Adversarial detection is a prevalent approach for achieving adversarial robustness. Rather than training victim policies to perform well in the presence of adversaries, adversarial detection focuses solely on detecting the existence of an adversary. In particular, we train an LSTM encoder [74] using (1) joint local observations, (2) joint actions, and (3) global state of a full episode, employing the representation at each

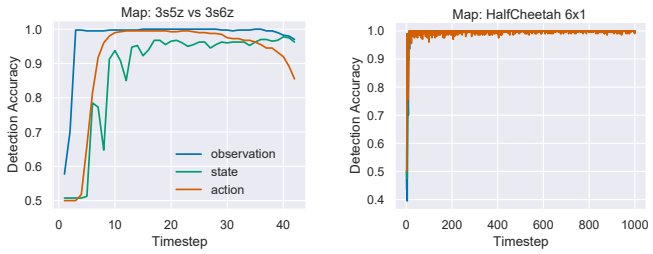

(a) SMAC environment (b) MAMujoco environment

Fig. 16: Adversarial detection. The presence of our AMI adversarial agent can be detected easily via using a classifier trained by observation, state or action. Adversary gets easier to detect as time proceeds.

timestep for binary prediction (*i.e.*, attack/no attack). For the sake of generality, we compile a database consisting of 100 game episodes without attack and 100 game episodes with attacks using the method of *Gleaves et al.*, train our classifier on this database, and assess whether the classifier can detect potential AMI attacks at each timestep. This approach enables us to evaluate the detection's generalizability to unseen attacks, rather than overfitting to attack-specific patterns. The results presented in Table. 16 lead us to several conclusions:

(1) AMI can be detected with high accuracy ($\geq 95\%$) using observations, states, or actions. This phenomenon is similar to the results reported by *Gleaves et al.*: while the policy taken by adversarial agents are harmful, they have to make large changes in policy to fool victims sufficiently. Furthermore, high detection accuracy can be attained as early as the 3^{rd} timestep for SMAC and the 12^{th} timestep for MAMujoco, demonstrating the potential to identify this attack at an early stage. *However, even knowing which agent is the adversary, defending against our attack could still be challenging and might necessitate human intervention.*

(2) The accuracy of adversarial detection improves over time. As the adversary executes sequential adversarial actions to influence the victim, our classifier gathers more evidence to determine if the current status contains an adversary. A notable exception is the use of joint actions as input in the SMAC environment. In the StarCraft game, most agents perish towards the end of the battle. These deceased agents take a specific action to signal their demise, generating similar input that confuses the classifier.

VII. Conclusion and Future Work

In this paper, we present AMI as a strong and practical black-box attack to assess the robustness of c-MARL, in which the attacker unilaterally influences victims to establish a worst-case collaboration. Firstly, we adapt agent-wise bilateral mutual information to a unilateral adversary-victim influence for policy-based attacks by decomposing mutual information and filtering out the influence from victims to the adversary. Secondly, we employ a reinforcement learning agent to generate the jointly worst-case target for the attacker to influence in order to maximize team reward. Through AMI, we pioneers the successful execution of adversarial attacks on real-world robotic swarms, and demonstrate its effectiveness in compelling agents towards collectively unfavorable outcomes in simulated environments. Our findings not only offer valuable insights into system vulnerabilities but also open opportunities to strengthen the resilience of cooperative multi-agent systems.

Despite demonstrating promising attack capabilities, there are several directions for further exploration. First, while AMI does not necessitate access to victim parameters and observations, it still requires millions of iterations interacting with victim agents to launch a successful attack, which may not be feasible in the real world. We aim to enhance the transferability and generalization capacity of our AMI attack, allowing attackers to train AMI in a simulated environment with surrogate victim policies and achieve high attack capability when directly deploying the policy in the real world. Second, we have observed that adversarial training techniques cannot consistently defend against our AMI attack. In the near future, we will address the unique robustness challenges and propose defense algorithms against our AMI attack. Lastly, as an initial exploration of c-MARL agents, we plan to extend our AMI attack to mixed cooperative-competitive games in future research.

VIII. Ethics Statement

While cooperative multi-agent reinforcement learning (c-MARL) has been extensively employed in a variety of applications, such as traffic light control [6], distributed resource allocation [7], and cooperative swarm control [9]–[11], evaluating its robustness and assessing its worst-case performance becomes a critical issue before real world deployment of such systems. While our proposed AMI attack can be harmful for c-MARL, it also serves benign purpose, which helps serves as a testing algorithm to evaluate the robustness of c-MARL. To mitigate the potentially harmful use of AMI, we propose several countermeasures against AMI attacks, but find them insufficiently effective due to the inherent complexity of c-MARL, further underscoring the urgent need for robust c-MARL policy defenses. In this way, our attack also urge the development of practical defense algorithms for c-MARL, which is crucial for the real world deployment of c-MARL. All experiments have been conducted using publicly available, open-source simulation environments and laboratory robotic environments, without involving human subjects or sensitive data.

IX. Acknowledgements

The author would like to thank Prof. Yaodong Yang for helpful discussion. This work was supported by the National Key Research and Development Plan of China (2021ZD0110601), the National Natural Science Foundation of China (62022009 and 62206009), and the State Key Laboratory of Software Development Environment. The writing was polished by GPT-4 [75].

REFERENCES

[1] Y. Yang and J. Wang, "An overview of multi-agent reinforcement learning from game theoretical perspective," *arXiv preprint arXiv:2011.00583*, 2020.

[2] B. Kiumarsi, K. G. Vamvoudakis, H. Modares, and F. L. Lewis, "Optimal and autonomous control using reinforcement learning: A survey," *IEEE transactions on neural networks and learning systems*, vol. 29, no. 6, pp. 2042–2062, 2017.

[3] H. Wang, Y. Yu, and Y. Jiang, "Fully decentralized multiagent communication via causal inference," *IEEE Transactions on Neural Networks and Learning Systems*, 2022.

[4] Z. Yang, K. Merrick, L. Jin, and H. A. Abbass, "Hierarchical deep reinforcement learning for continuous action control," *IEEE transactions on neural networks and learning systems*, vol. 29, no. 11, pp. 5174–5184, 2018.

[5] M. Samvelyan, T. Rashid, C. S. De Witt, G. Farquhar, N. Nardelli, T. G. Rudner, C.-M. Hung, P. H. Torr, J. Foerster, and S. Whiteson, "The starcraft multi-agent challenge," *arXiv preprint arXiv:1902.04043*, 2019.

[6] T. Wu, P. Zhou, K. Liu, Y. Yuan, X. Wang, H. Huang, and D. O. Wu, "Multi-agent deep reinforcement learning for urban traffic light control in vehicular networks," *IEEE Transactions on Vehicular Technology*, vol. 69, no. 8, pp. 8243–8256, 2020.

[7] C. Zhang, V. Lesser, and P. Shenoy, "A multi-agent learning approach to online distributed resource allocation," in *Twenty-first international joint conference on artificial intelligence*, 2009.

[8] Y. Jiang and Z.-P. Jiang, "Robust adaptive dynamic programming with an application to power systems," *IEEE Transactions on Neural Networks and Learning Systems*, vol. 24, no. 7, pp. 1150–1156, 2013.

[9] B. Peng, T. Rashid, C. Schroeder de Witt, P.-A. Kamienny, P. Torr, W. Böhmer, and S. Whiteson, "Facmac: Factored multi-agent centralised policy gradients," *Advances in Neural Information Processing Systems*, vol. 34, pp. 12 208–12 221, 2021.

[10] M. Hüttenrauch, S. Adrian, G. Neumann *et al.*, "Deep reinforcement learning for swarm systems," *Journal of Machine Learning Research*, vol. 20, no. 54, pp. 1–31, 2019.

[11] W. J. Yun, S. Park, J. Kim, M. Shin, S. Jung, D. A. Mohaisen, and J.-H. Kim, "Cooperative multiagent deep reinforcement learning for reliable surveillance via autonomous multi-uav control," *IEEE Transactions on Industrial Informatics*, vol. 18, no. 10, pp. 7086–7096, 2022.

[12] J. Lin, K. Dzeparoska, S. Q. Zhang, A. Leon-Garcia, and N. Papernot, "On the robustness of cooperative multi-agent reinforcement learning," in *2020 IEEE Security and Privacy Workshops (SPW)*. IEEE, 2020, pp. 62–68.

[13] S. Huang, N. Papernot, I. Goodfellow, Y. Duan, and P. Abbeel, "Adversarial attacks on neural network policies," *arXiv preprint arXiv:1702.02284*, 2017.

[14] H. Zhang, H. Chen, C. Xiao, B. Li, M. Liu, D. Boning, and C.-J. Hsieh, "Robust deep reinforcement learning against adversarial perturbations on state observations," *Advances in Neural Information Processing Systems*, vol. 33, pp. 21 024–21 037, 2020.

[15] A. Gleave, M. Dennis, C. Wild, N. Kant, S. Levine, and S. Russell, "Adversarial policies: Attacking deep reinforcement learning," *arXiv preprint arXiv:1905.10615*, 2019.

[16] X. Wu, W. Guo, H. Wei, and X. Xing, "Adversarial policy training against deep reinforcement learning," in *30th USENIX Security Symposium (USENIX Security 21)*, 2021, pp. 1883–1900.

[17] W. Guo, X. Wu, S. Huang, and X. Xing, "Adversarial policy learning in two-player competitive games," in *International Conference on Machine Learning*. PMLR, 2021, pp. 3910–3919.

[18] J. Wu and X. Xu, "Decentralised grid scheduling approach based on multi-agent reinforcement learning and gossip mechanism," *CAAI Transactions on Intelligence Technology*, vol. 3, no. 1, pp. 8–17, 2018.

[19] D. Ye, M. Zhang, and Y. Yang, "A multi-agent framework for packet routing in wireless sensor networks," *sensors*, vol. 15, no. 5, pp. 10 026–10 047, 2015.

[20] N. Dandanov, H. Al-Shatri, A. Klein, and V. Poulkov, "Dynamic self-optimization of the antenna tilt for best trade-off between coverage and capacity in mobile networks," *Wireless Personal Communications*, vol. 92, no. 1, pp. 251–278, 2017.

[21] S. Shalev-Shwartz, S. Shammah, and A. Shashua, "Safe, multi-agent, reinforcement learning for autonomous driving," *arXiv preprint arXiv:1610.03295*, 2016.

[22] S. Bhalla, S. Ganapathi Subramanian, and M. Crowley, "Deep multi agent reinforcement learning for autonomous driving," in *Canadian Conference on Artificial Intelligence*. Springer, 2020, pp. 67–78.

[23] M. Zhou, J. Luo, J. Villella, Y. Yang, D. Rusu, J. Miao, W. Zhang, M. Alban, I. Fadakar, Z. Chen *et al.*, "Smarts: Scalable multi-agent reinforcement learning training school for autonomous driving," *arXiv preprint arXiv:2010.09776*, 2020.

[24] P. Palanisamy, "Multi-agent connected autonomous driving using deep reinforcement learning," in *2020 International Joint Conference on Neural Networks (IJCNN)*. IEEE, 2020, pp. 1–7.

[25] A. Gardikiotis, "Minority influence," *Social and personality psychology compass*, vol. 5, no. 9, pp. 679–693, 2011.

[26] C. Szegedy, W. Zaremba, I. Sutskever, J. Bruna, D. Erhan, I. Goodfellow, and R. Fergus, "Intriguing properties of neural networks," *arXiv preprint arXiv:1312.6199*, 2013.

[27] I. J. Goodfellow, J. Shlens, and C. Szegedy, "Explaining and harnessing adversarial examples," *arXiv preprint arXiv:1412.6572*, 2014.

[28] N. Carlini and D. Wagner, "Towards evaluating the robustness of neural networks," in *2017 ieee symposium on security and privacy (sp)*. IEEE, 2017, pp. 39–57.

[29] J. Kos and D. Song, "Delving into adversarial attacks on deep policies," *arXiv preprint arXiv:1705.06452*, 2017.

[30] Y.-C. Lin, Z.-W. Hong, Y.-H. Liao, M.-L. Shih, M.-Y. Liu, and M. Sun, "Tactics of adversarial attack on deep reinforcement learning agents," *arXiv preprint arXiv:1703.06748*, 2017.

[31] Y. Huang and Q. Zhu, "Deceptive reinforcement learning under adversarial manipulations on cost signals," in *International Conference on Decision and Game Theory for Security*. Springer, 2019, pp. 217–237.

[32] A. Rakhsha, G. Radanovic, R. Devidze, X. Zhu, and A. Singla, "Policy teaching via environment poisoning: Training-time adversarial attacks against reinforcement learning," in *International Conference on Machine Learning*. PMLR, 2020, pp. 7974–7984.

[33] F. Wu, L. Li, C. Xu, H. Zhang, B. Kailkhura, K. Kenthapadi, D. Zhao, and B. Li, "Copa: Certifying robust policies for offline reinforcement learning against poisoning attacks," *arXiv preprint arXiv:2203.08398*, 2022.

[34] V. Behzadan and W. Hsu, "Sequential triggers for watermarking of deep reinforcement learning policies," *arXiv preprint arXiv:1906.01126*, 2019.

[35] L. Wang, Z. Javed, X. Wu, W. Guo, X. Xing, and D. Song, "Backdoorl: Backdoor attack against competitive reinforcement learning," *arXiv preprint arXiv:2105.00579*, 2021.

[36] P. Kiourti, K. Wardega, S. Jha, and W. Li, "Trojdrl: Trojan attacks on deep reinforcement learning agents," *arXiv preprint arXiv:1903.06638*, 2019.

[37] Z. Yang, N. Iyer, J. Reimann, and N. Virani, "Design of intentional backdoors in sequential models," *arXiv preprint arXiv:1902.09972*, 2019.

[38] H. Zhang, H. Chen, D. Boning, and C.-J. Hsieh, "Robust reinforcement learning on state observations with learned optimal adversary," *arXiv preprint arXiv:2101.08452*, 2021.

[39] Y. Sun, R. Zheng, Y. Liang, and F. Huang, "Who is the strongest enemy? towards optimal and efficient evasion attacks in deep rl," *arXiv preprint arXiv:2106.05087*, 2021.

[40] N. Papernot, P. McDaniel, S. Jha, M. Fredrikson, Z. B. Celik, and A. Swami, "The limitations of deep learning in adversarial settings," in *2016 IEEE European symposium on security and privacy (EuroS&P)*. IEEE, 2016, pp. 372–387.

[41] J. Tu, T. Wang, J. Wang, S. Manivasagam, M. Ren, and R. Urtasun, "Adversarial attacks on multi-agent communication," in *Proceedings of the IEEE/CVF International Conference on Computer Vision*, 2021, pp. 7768–7777.

[42] W. Xue, W. Qiu, B. An, Z. Rabinovich, S. Obraztsova, and C. K. Yeo, "Mis-spoke or mis-lead: Achieving robustness in multi-agent communicative reinforcement learning," *arXiv preprint arXiv:2108.03803*, 2021.

[43] J. Blumenkamp and A. Prorok, "The emergence of adversarial communication in multi-agent reinforcement learning," in *Conference on Robot Learning*. PMLR, 2021, pp. 1394–1414.

[44] R. Mitchell, J. Blumenkamp, and A. Prorok, "Gaussian process based message filtering for robust multi-agent cooperation in the presence of adversarial communication," *arXiv preprint arXiv:2012.00508*, 2020.

[45] T. Rashid, M. Samvelyan, C. Schroeder, G. Farquhar, J. Foerster, and S. Whiteson, "Qmix: Monotonic value function factorisation for deep multi-agent reinforcement learning," in *International conference on machine learning*. PMLR, 2018, pp. 4295–4304.

[46] C. Yu, A. Velu, E. Vinitsky, Y. Wang, A. Bayen, and Y. Wu, "The surprising effectiveness of ppo in cooperative, multi-agent games," *arXiv preprint arXiv:2103.01955*, 2021.

[47] J. Foerster, G. Farquhar, T. Afouras, N. Nardelli, and S. Whiteson, "Counterfactual multi-agent policy gradients," in *Proceedings of the AAAI conference on artificial intelligence*, vol. 32, no. 1, 2018.

[48] R. Lowe, Y. I. Wu, A. Tamar, J. Harb, O. Pieter Abbeel, and I. Mordatch, "Multi-agent actor-critic for mixed cooperative-competitive environments," *Advances in neural information processing systems*, vol. 30, 2017.

[49] A. Tampuu, T. Matiisen, D. Kodelja, I. Kuzovkin, K. Korjus, J. Aru, J. Aru, and R. Vicente, "Multiagent cooperation and competition with deep reinforcement learning," *PloS one*, vol. 12, no. 4, p. e0172395, 2017.

[50] P. Sunehag, G. Lever, A. Gruslys, W. M. Czarnecki, V. Zambaldi, M. Jaderberg, M. Lanctot, N. Sonnerat, J. Z. Leibo, K. Tuyls *et al.*, "Value-decomposition networks for cooperative multi-agent learning," *arXiv preprint arXiv:1706.05296*, 2017.

[51] K. Son, D. Kim, W. J. Kang, D. E. Hostallero, and Y. Yi, "Qtran: Learning to factorize with transformation for cooperative multi-agent reinforcement learning," in *International conference on machine learning*. PMLR, 2019, pp. 5887–5896.

[52] J. Wang, Z. Ren, T. Liu, Y. Yu, and C. Zhang, "Qplex: Duplex dueling multi-agent q-learning," *arXiv preprint arXiv:2008.01062*, 2020.

[53] C. S. de Witt, T. Gupta, D. Makoviichuk, V. Makoviychuk, P. H. Torr, M. Sun, and S. Whiteson, "Is independent learning all you need in the starcraft multi-agent challenge?" *arXiv preprint arXiv:2011.09533*, 2020.

[54] N. Jaques, A. Lazaridou, E. Hughes, C. Gulcehre, P. Ortega, D. Strouse, J. Z. Leibo, and N. De Freitas, "Social influence as intrinsic motivation for multi-agent deep reinforcement learning," in *International conference on machine learning*. PMLR, 2019, pp. 3040–3049.

[55] T. Wang, J. Wang, Y. Wu, and C. Zhang, "Influence-based multi-agent exploration," *arXiv preprint arXiv:1910.05512*, 2019.

[56] W. Kim, W. Jung, M. Cho, and Y. Sung, "A maximum mutual information framework for multi-agent reinforcement learning," *arXiv preprint arXiv:2006.02732*, 2020.

[57] P. Li, H. Tang, T. Yang, X. Hao, T. Sang, Y. Zheng, J. Hao, M. E. Taylor, and Z. Wang, "Pmic: Improving multi-agent reinforcement learning with progressive mutual information collaboration," *arXiv preprint arXiv:2203.08553*, 2022.

[58] E. A. Hansen, D. S. Bernstein, and S. Zilberstein, "Dynamic programming for partially observable stochastic games," in *AAAI*, vol. 4, 2004, pp. 709–715.

[59] S. Höfer, K. Bekris, A. Handa, J. C. Gamboa, M. Mozifian, F. Golemo, C. Atkeson, D. Fox, K. Goldberg, J. Leonard *et al.*, "Sim2real in robotics and automation: Applications and challenges," *IEEE transactions on automation science and engineering*, vol. 18, no. 2, pp. 398–400, 2021.

[60] A. K. Sahu, S. Sharma, and D. Puthal, "Lightweight multi-party authentication and key agreement protocol in iot-based e-healthcare service," *ACM Transactions on Multimedia Computing, Communications, and Applications (TOMM)*, vol. 17, no. 2s, pp. 1–20, 2021.

[61] A. Y. Khan, R. Latif, S. Latif, S. Tahir, G. Batool, and T. Saba, "Malicious insider attack detection in iots using data analytics," *IEEE Access*, vol. 8, pp. 11 743–11 753, 2019.

[62] L. Zhang and Y.-C. Liang, "Deep reinforcement learning for multi-agent power control in heterogeneous networks," *IEEE Transactions on Wireless Communications*, vol. 20, no. 4, pp. 2551–2564, 2020.

[63] A. A. Khan and R. S. Adve, "Centralized and distributed deep reinforcement learning methods for downlink sum-rate optimization," *IEEE Transactions on Wireless Communications*, vol. 19, no. 12, pp. 8410–8426, 2020.

[64] S. M. Giray, "Anatomy of unmanned aerial vehicle hijacking with signal spoofing," in *2013 6th International Conference on Recent Advances in Space Technologies (RAST)*. IEEE, 2013, pp. 795–800.

[65] B. Ly and R. Ly, "Cybersecurity in unmanned aerial vehicles (uavs)," *Journal of Cyber Security Technology*, vol. 5, no. 2, pp. 120–137, 2021.

[66] N. M. Rodday, R. d. O. Schmidt, and A. Pras, "Exploring security vulnerabilities of unmanned aerial vehicles," in *NOMS 2016-2016 IEEE/IFIP Network Operations and Management Symposium*. IEEE, 2016, pp. 993–994.

[67] K. Kuru, D. Ansell, W. Khan, and H. Yetgin, "Analysis and optimization of unmanned aerial vehicle swarms in logistics: An intelligent delivery platform," *Ieee Access*, vol. 7, pp. 15 804–15 831, 2019.

[68] J. Guo, Y. Chen, Y. Hao, Z. Yin, Y. Yu, and S. Li, "Towards comprehensive testing on the robustness of cooperative multi-agent reinforcement learning," in *Proceedings of the IEEE/CVF Conference on Computer Vision and Pattern Recognition*, 2022, pp. 115–122.

[69] W. D. Crano and V. Seyranian, "Majority and minority influence," *Social and Personality Psychology Compass*, vol. 1, no. 1, pp. 572–589, 2007.

[70] A. Fayad and M. Ibrahim, "Influence-based reinforcement learning for intrinsically-motivated agents," *arXiv preprint arXiv:2108.12581*, 2021.

[71] J. Schulman, F. Wolski, P. Dhariwal, A. Radford, and O. Klimov, "Proximal policy optimization algorithms," *arXiv preprint arXiv:1707.06347*, 2017.

[72] J. Schulman, P. Moritz, S. Levine, M. Jordan, and P. Abbeel, "High-dimensional continuous control using generalized advantage estimation," *arXiv preprint arXiv:1506.02438*, 2015.

[73] F. Mondada, M. Bonani, X. Raemy, J. Pugh, C. Cianci, A. Klaptocz, S. Magnenat, J.-C. Zufferey, D. Floreano, and A. Martinoli, "The e-puck, a robot designed for education in engineering," in *Proceedings of the 9th conference on autonomous robot systems and competitions*, vol. 1, no. CONF. IPCB: Instituto Politécnico de Castelo Branco, 2009, pp. 59–65.

[74] S. Hochreiter and J. Schmidhuber, "Long short-term memory," *Neural computation*, vol. 9, no. 8, pp. 1735–1780, 1997.

[75] S. Bubeck, V. Chandrasekaran, R. Eldan, J. Gehrke, E. Horvitz, E. Kamar, P. Lee, Y. T. Lee, Y. Li, S. Lundberg *et al.*, "Sparks of artificial general intelligence: Early experiments with gpt-4," *arXiv preprint arXiv:2303.12712*, 2023.

[76] G. Papoudakis, F. Christianos, L. Schäfer, and S. V. Albrecht, "Benchmarking multi-agent deep reinforcement learning algorithms in cooperative tasks," *arXiv preprint arXiv:2006.07869*, 2020.

[77] E. Todorov, T. Erez, and Y. Tassa, "Mujoco: A physics engine for model-based control," in *2012 IEEE/RSJ international conference on intelligent robots and systems*. IEEE, 2012, pp. 5026–5033.

[78] J. G. Kuba, R. Chen, M. Wen, Y. Wen, F. Sun, J. Wang, and Y. Yang, "Trust region policy optimisation in multi-agent reinforcement learning," *arXiv preprint arXiv:2109.11251*, 2021.

[79] F. A. Salem, "Dynamic and kinematic models and control for differential drive mobile robots," *International Journal of Current Engineering and Technology*, vol. 3, no. 2, pp. 253–263, 2013.

APPENDIX

I. MORE DETAILS OF AMI METHOD

A. More Details of Eqn. 6

We start from $-D_{KL}\left(\mathbb{E}_{\tilde{a}_t^\alpha\sim\pi_t^\alpha}\left[p_\phi(\hat{a}_{t+1,i}^\nu|s_t,\tilde{a}_t^\alpha,\mathbf{a}_t^\nu)\right]||\,\mathcal{U}\right)$, which can be expressesd as:

$$
\begin{aligned}
&-D_{KL}\left(\mathbb{E}_{\tilde{a}_t^\alpha\sim\pi_t^\alpha}\left[p_\phi(\hat{a}_{t+1,i}^\nu|s_t,\tilde{a}_t^\alpha,\mathbf{a}_t^\nu)\right]||\,\mathcal{U}\right)\\
=&-D_{KL}\left(\left[\sum_{\tilde{a}_t^\alpha}p_\phi(\hat{a}_{t+1,i}^\nu|s_t,\tilde{a}_t^\alpha,\mathbf{a}_t^\nu)\cdot p_\theta(\tilde{a}_t^\alpha|s_t,\mathbf{a}_t^\nu)\right]||\,\mathcal{U}\right),\\
=&-D_{KL}\left(\left[\sum_{\tilde{a}_t^\alpha}p_\phi(\hat{a}_{t+1,i}^\nu|s_t,\tilde{a}_t^\alpha,\mathbf{a}_t^\nu)\cdot p_\theta(\tilde{a}_t^\alpha|s_t)\right]||\,\mathcal{U}\right),\\
=&-D_{KL}\left(p_\phi(\hat{a}_{t+1,i}^\nu|s_t,\mathbf{a}_t^\nu)||\,\mathcal{U}\right),\\
=&-\sum_{\hat{a}_{t+1,i}\in\mathcal{A}_i}p_\phi(\hat{a}_{t+1,i}^\nu|s_t,\mathbf{a}_t^\nu)\log\left(\frac{p_\phi(\hat{a}_{t+1,i}^\nu|s_t,\mathbf{a}_t^\nu)}{\mathcal{U}}\right),\\
=&-\sum_{\hat{a}_{t+1,i}\in\mathcal{A}_i}p_\phi(\hat{a}_{t+1,i}^\nu|s_t,\mathbf{a}_t^\nu)\log\left(p_\phi(\hat{a}_{t+1,i}^\nu|s_t,\mathbf{a}_t^\nu)-\right.\\
&\qquad\left.p_\phi(\hat{a}_{t+1,i}^\nu|s_t,\mathbf{a}_t^\nu)\log(\mathcal{U}),\right.\\
=&-\sum_{\hat{a}_{t+1,i}\in\mathcal{A}_i}p_\phi(\hat{a}_{t+1,i}^\nu|s_t,\mathbf{a}_t^\nu)\log\left(p_\phi(\hat{a}_{t+1,i}^\nu|s_t,\mathbf{a}_t^\nu)\right)-c,\\
=&H(\hat{a}_{t+1,i}^\nu|s_t,\mathbf{a}_t^\nu)-c.
\end{aligned}
\tag{10}
$$

Moving $-c$ to other side completes our claim in Fig. 6, where c is a constant irrelevant to our attack. The derivation comes from standard definition of KL divergence and information theory, which indicates that maximizing minority influence is equal to minimizing the KL divergence between victim. The derivation of Eqn. 6 in continuous setting is the same as discrete setting, since the logarithm of uniform distribution $\mathcal{U}$ is always a constant.

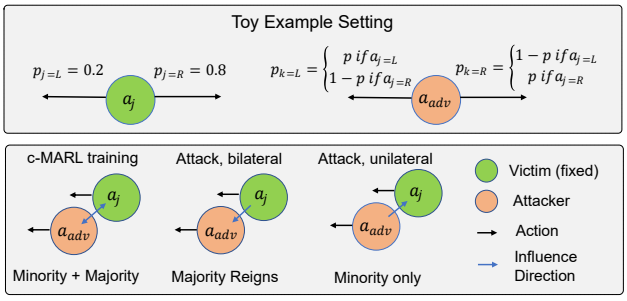

Fig. A1: Toy example used to illustrate our majority and minority influence theme. In this toy example, the adversary a_{adv} tries to influence the policy of a fixed victim agent a_j. While the a_{adv} cannot actually influence the policy of a_j, using allows a_{adv} to cheat by changing its own policy that fits to the policy of a_j.

B. Majority and Minority Influence

Next, we use a toy example to motivate our claim in main paper. Under this toy example, we can calculate mutual information and optimal policy analytically. Specifically, the experiment setting is illustrated in Fig. A1. In this experiment, we assume two agents exists, the adversary a_{adv} and a victim agent a_j with fixed policy. Both agents can only take actions to go left or right. The policy of victim agent a_j is fixed, such that it goes left at probability 0.2 and right at probability 0.8, while the policy of adversary agent a_{adv} can be adapted for attack. Its policy is conditioned on the action taken by victim, where we omit temporal dependence for simplicity, while the only parameter it can control is the probability p, such that its probability of going left or right adapts to victim action. The task of adversary a_{adv} is to change influence the action probability of victim a_j. However, since the policy of victim agent a_j is fixed, it is actually impossible for a_{adv} to influence a_j.

As a consequence, a proper influence metric should also reflect this property, such that no matter how p changes, it is impossible to gain influence by changing p controlled by a_{adv} to affect a_j. However, in mutual information, this is not the case. As shown in Fig. A2a, the adversary can actually affect mutual information $I(a_j;a_{adv})$ by changing its own action probability p. While the probability of $p(a_j)$ is fixed, calculating mutual information relies on the joint action probability $p(a_j,a_{adv})$, leaving space for adversary to change its action probability that influence mutual information. Specifically, to be maximally informative of a_j, a_{adv} can change its policy to be maximally predictive of a_j. Thus, adversary maximize its mutual information between itself and victim by overfitting to the policy of victim.

We shall note that this problem is unique to policy-based attack since the victim policy is fixed. As the number of agent increases, changing the action of one agent creates less impact on fixed victim parameter, such that victim will yield increasingly fixed policy (*i.e.*, action probability). However, in common c-MARL training, since all agents can adapt their policy jointly, such unexpected behavior do not exist in mutual information.

To solve this problem, note that mutual information $I(a_j;a_{adv}) = -H(a_j|a_{adv}) + H(a_j)$, where the former indicates majority influence and the latter is minority influence. As illustrated in Fig. A2b, and Fig. A2c, majority influence is the major source for adversary to change its own policy to overfit the adversary. However, minority influence term is free of such problem. No matter how adversary change its policy p, the magnitude of influence stays still. As a consequence, attacker cannot cheat for higher influence by changing its policy, since the reward gained remains constant.

II. MORE DETAILS OF SIMULATION ENVIRONMENTS

In this section, we introduce the environments we attack for simulation (SMAC and MAMujoco) in detail. Specifically, we introduce the environment, adversary reward, evaluation metric, and detailed attack settings.

A. SMAC environment

1) Introduction: StarCraftII Multi-Agent Challenge environment [5] is a widely used discrete-action environment for evaluating the effectiveness of multi-agent reinforcement learning. In SMAC, each agent can select one discrete action

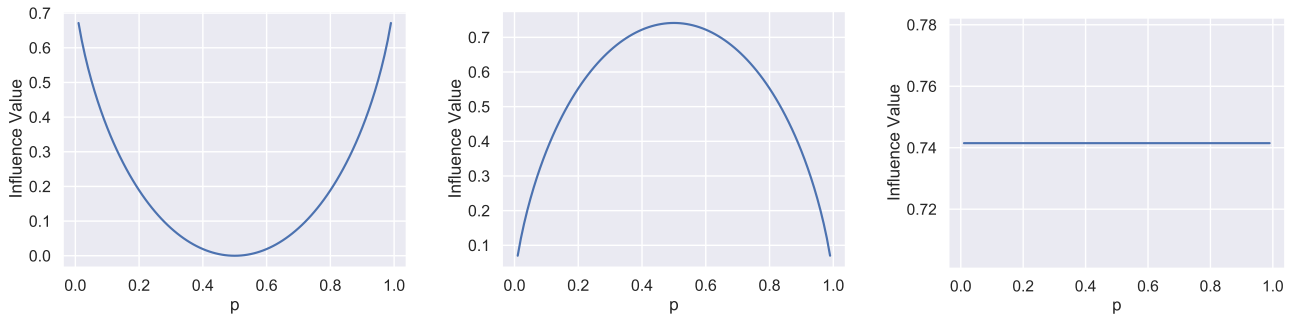

(a) Mutual Information (b) Majority Influence (c) Minority Influence

Fig. A2: The mutual information, majority influence and minority influence calculated in our toy example. In mutual information, adversary is able to maximize its influence by changing its policy p, without actually changing the action probability of a_j. This unexpected behavior originates in majority influence term in mutual information, and is not expressed in minority influence.

available at the current timestep, including moving and attacking. Specifically, we base our framework on Extended Pymarl [76], an extended version of the original code described in [5] widely used to evaluate the performance of SMAC.

2) Adversary Reward: In the original version of SMAC [5], agents were trained using a *shaped reward* of enemies, which we call it (*reward_enemies*). This reward contains three terms: (1) hit-point damage dealt to enemies. (2) enemy units killed. (3) winning the game. However, we argue this reward cannot comprehensively evaluate the attack performance of the attacker, since the goal of the attacker is to affect its allies, while the only loss in enemies is counted. To comprehensively evaluate the attack performance of the adversary, we argue that loss in both enemies and allies should be considered. We add a symmetric version of *shaped allies reward* (*reward_allies*) that measures the exact three terms just like enemies: (1) hit-point damage dealt to allies. (2) ally units killed. (3) losing the game. Finally, adversary reward is defined as *reward_enemies* - *reward_allies* and used for AMI and all other baselines.

3) Evaluation metric: After proposing our adversarial reward, we believe the winning rate is insufficient to evaluate attacker capability in SMAC environment. While original SMAC tasks seek to maximize the rate of winning, the goal of the attacker is to not only fool allies towards a failure (losing the game), but also to minimize the loss of enemies and maximize the loss of victims. It is possible that both adversary can fool victims to a winning rate of 0, but one adversary is better by additionally good at reducing the number of death of enemies. Clearly, to reduce enemy death, adversary must learn a smarter way to influence its victims to achieve this stronger result. This motivates us to use our adversarial reward to evaluate attack effort more comprehensively.

4) Detailed attack setting: SMAC environments differ from MAMujoco that victims combat with another group of enemies. Originally, two groups of agents have similar combat capabilities. However, the introduction of an attacker itself weakens the combat capability of victims even if we do not use adversarial policy. This leads to an unfair battle (for example, victims can never win in *10m vs 11m* environment if one ally is controlled by the attacker, resulting in 9 marines controlled by MARL to combat with 11 marines controlled by heuristic AI). To fairly evaluate attacks in SMAC environment, we add an adversarial agent to the side of victims, train all victims together, then use adversarial policy to attack that added agent.

B. MAMujoco environment

1) Introduction: Mujoco [77] is a well-known environment where robots learn to control their joints to move in an optimal way. Multi-agent Mujoco environment [9] implements Mujoco in a multi-agent fashion, where the original robot was separated into independent parts, and the goal is to learn a strategy to move cooperatively in an optimal way. We base our framework for MAMujoco on the implementation of [78], which implements MAPPO with high performance. We use the default hyperparameters in their implementations without modification.

2) Adversary Reward: The reward of MAMujoco is similar compared with Mujoco, which contains two terms, *reward_run* and *reward_ctrl*. *reward_run* specifies the reward for robots achieving high forward velocity; while *reward_ctrl* penalizes the robot for having large a action vector magnitude. We define adversary reward as the negative of *reward_run*, since *reward_ctrl* is an auxiliary reward used in normal training and does not reflect the concern of the adversary.

III. More Details of Baseline Implementations

For all baselines, we train them to maximize the adversary reward given above, adapting their method to c-MARL attack while maximally following their originally proposed methods. (1) For the method of *Guo et al.* [17], we add a central critic to estimate and minimize victim rewards, as described by their method. (2) For the method of *Wu et al.* [16], since their method is proposed for continuous control only, in continuous control, we implement their action prediction module (Eqn. 12 in their original paper) by cross-entropy loss. (3) For the observation-based attack of *Lin et al.* [12], we follow their default implementation and set the maximum attack iteration to 30. The perturbation budget is measured by ℓ_∞ norm.

IV. More Details of Real-World Robot Environments

In this section, we describe the details of real-world robot environments.

A. Real-world environment

We perform all experiments based on a set of e-puck2 robot [73], a mini mobile robot developed by EPFL, which is a widely used robot in various research and educational scenarios. We added an expansion board with Raspberry Pi to E-puck2 robots to increase their computing power.

The experiments take place in a 2m $\times$ 2m indoor arena, with walls on the boundary. We add a centralized motion capture system to capture the position of each robot, such that we can calculate the state and observation information required by [10]. To fairly compare each method and avoid the effect of initialization, in each runs (we tested all methods for 10 runs), we initialize all methods to the same position (we project the place for initialization using the blue cross projected in our arena, as shown in Fig. 4b in our main paper. Then, we manually place all robots to the projected blue cross before the episode starts), while the initialization varies among different experiment runs. This corresponds to a *within-subjects* design, so we test our result using the corresponding paired samples t-test and Wilcoxon signed-rank test, respectively.

B. Task and reward

We conduct our simulation experiment in a rendezvous environment following the work [10]. In this environment, all robots were encouraged to meet in the same location to get the highest reward. The location can be an arbitrary valid location in the map. The reward contains two parts, *reward_distance* (r_d), which specifies how robots were close to each other. Similar to Mujoco [77], a penalty term *reward_control* (r_c) was added as the L2 norm of the action each agents, in order to to penalize extremely large actions. The full reward r can be expressed as:

$$r = r_d - 0.001 \cdot r_c. \tag{11}$$

To encourage robots close to each other, *reward_distance* can be expressed as:

$$r_d = -\sum_{i=0}^{N} \sum_{j=i+1}^{N} ||\mathbf{p}_i - \mathbf{p}_j||_2, \tag{12}$$

where $\mathbf{p} = (x, y)$ is the point that contains the x and y position of the current robot, N is the number of robots. Under this reward, each robot receives larger reward for being closer to each other.

As the L2 norm of actions, *reward_control* can be expressed as:

$$r_c = \sum_{i=0}^{N} ||\mathbf{a}_i||_2, \tag{13}$$

where $\mathbf{a}_i$ is the action taken by all individual robots.

C. Observation and Actions

To measure and convey information of all robots, we maintain two global matrices which we use to get local and global observations: distance matrix (M_d) and angle matrix (M_a).

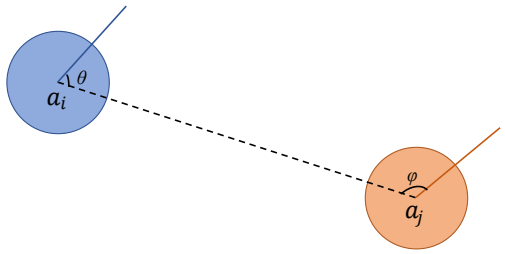

Fig. A3: The definition of angles in angle matrix M_a. Blue and orange circles a_i, a_j refer to the target robot and another robot, the solid line indicates the orientation of robots. θ is at the i-th row and j-th column of M_a, and φ is at the j-th row and i-th column of M_a.

Each element in the distance matrix represents the Euclidean distance between two robots. As for the angle in M_a, we calculate the pairwise included angle between every two agents. As illustrated in Fig. A3, to calculate the included angle θ of a_i comparing with a_j, the angle is calculated between the line connecting a_i and a_j and the current orientation of a_i.

The **observations** of each agents can then be calculated from M_d and M_a, which contains the distance with other agents, and 4 included angle between two agents, which can be calculated from M_a: $\cos\theta$, $\sin\theta$, $\cos\varphi$ and $\sin\varphi$. The global state s^t contains the distance and angle between each individual agent:

$$\begin{aligned} s^t &= \{M_d^t, M_a^t\} \\ &= \{M_d^t, \theta^t, \varphi^t\}. \end{aligned} \tag{14}$$

The local observation o^t contains the distance and the sine and cosine value of the angle between the local agent and all other agents:

$$o_i^t = \{M_{d,i}^t, \sin\theta_i^t, \cos\theta_i^t, \sin\varphi_i^t, \cos\varphi_i^t\}. \tag{15}$$

The **action** of the environments includes the angular velocity of two wheels of robots. The orientation of the robot is controlled by the difference of wheel velocity, driven by differential drive kinematics [79].

V. Experiment Hyperparameters

In this section, we describe the hyperparameters of AMI and baselines. For **SMAC environment**, Table. A1 describes the shared parameters used by all methods in SMAC experiments. Table. A2 denotes the hyperparameters used for each individual methods.

For **MAMujoco environment**, Table. A3 describes the parameters used for all experiments. Table. A4 denotes the hyperparameters used for each individual methods.

For **rendezvous environment**, the hyperparameters and implementations follows MAMujoco environment, with small variations to achieve best performance in this scenario. Table. A5 describes the parameters used for the rendezvous environment. Table. A6 denotes the hyperparameters used for each individual methods.

TABLE A1: Shared hyperparameters for SMAC, used in AMI and all baselines.

Hyperparameter	Value	Hyperparameter	Value
lr	1e-4	mini-batch num	1
parallel envs	32	max grad norm	10
gamma	0.99	max episode len	150
actor network	mlp	actor lr	=lr
hidden dim	64	critic lr	=lr
hidden layer	1	PPO epoch	4
activation	ReLU	PPO clip	0.2
optimizer	Adam	entropy coef	0.01
GAE lambda	0.95	eval episode	20

TABLE A2: Method-specific parameters for *Wu et al.*, *Guo et al.* and our AMI in SMAC environment.

Hyperparameters for Wu et al.			
Hyperparameter	Value	Hyperparameter	Value
epsilon_state	0.1	epsilon_action	0.1
lr_state	=actor lr	lr_action	=actor lr
Hyperparameters for *Guo et al.*			
Hyperparameter	Value	Hyperparameter	Value
victim critic lr	=lr		
Hyperparameters for AMI			
Hyperparameter	Value	Hyperparameter	Value
p_ϕ lr	=lr	TAO lr	=lr
TAO critic lr	=lr	AMI lambda	[.03, .05, .1]

TABLE A3: Shared hyperparameters for MAMujoco, used in AMI and all baselines in MAMujoco environment.

Hyperparameter	Value	Hyperparameter	Value
parallel envs	32	mini-batch num	40
gamma	0.99	max grad norm	10
gain	0.01	max episode len	1000
actor network	mlp	actor lr	[5e-6, 5e-4]
std y coef	0.5	critic lr	5e-3
std x coef	1	Huber loss	True
hidden dim	64	Huber delta	10
hidden layer	1	PPO epoch	5
activation	ReLU	PPO clip	0.2
optimizer	Adam	entropy coef	0.01
GAE lambda	0.95	eval episode	32

TABLE A4: Method-specific parameters for *Wu et al.*, *Guo et al.* and our AMI in MAMujoco environment.

Hyperparameters for Wu et al.			
Hyperparameter	Value	Hyperparameter	Value
epsilon_state	0.1	epsilon_action	0.1
lr_state	=actor lr	lr_action	=actor lr
Hyperparameters for *Guo et al.*			
Hyperparameter	Value	Hyperparameter	Value
victim critic lr	=lr		
Hyperparameters for AMI			
Hyperparameter	Value	Hyperparameter	Value
p_ϕ lr	=lr	TAO lr	=lr
TAO critic lr	=lr	AMI lambda	[.01, .1, .3, 1]

TABLE A5: Shared hyperparameters for rendezvous, used in AMI and all baselines.

Hyperparameter	Value	Hyperparameter	Value
parallel envs	32	mini-batch num	40
gamma	0.99	max grad norm	10
gain	0.01	max episode len	1000
actor network	mlp	actor lr	5e-5
std y coef	0.5	critic lr	5e-3
std x coef	1	Huber loss	True
hidden dim	64	Huber delta	10
hidden layer	1	PPO epoch	5
activation	ReLU	PPO clip	0.2
optimizer	Adam	entropy coef	0.01
GAE lambda	0.95	eval episode	32

VI. AMI Attack in Different Positions

Besides attacking agents in different environments, due to the heterogeneity of c-MARL, agents with different IDs might have different initial positions and utility. This fact motivates us to verify if AMI is also effective when attacking agents with different initialization and functionalities. Specifically, we test AMI in *3s5z vs 3s6z* environment in SMAC, with results shown in Fig. A4. In each subfigure, adversary controls an agent with different IDs, resulting in different initialize positions and functions (as long-range Stalker or short-range Zealot). It is worth noting that in our experiment setting, we add a zealot in the left side of agents to counter the negative effect brought by the adversary, resulting in three stalkers and six zealots. Note that the attack result on agent 1 (Stalker) already illustrated in Fig. 7. Clearly, the performance of AMI is stable under different initialization and functionalities, achieving better result on 8 over 9 attack positions.

TABLE A6: Method-specific parameters for *Wu et al.*, *Guo et al.* and our AMI in rendezvous environment.

Hyperparameters for Wu et al.			
Hyperparameter	Value	Hyperparameter	Value
epsilon_state	0.1	epsilon_action	0.1
lr_state	=actor lr	lr_action	=actor lr
Hyperparameters for *Guo et al.*			
Hyperparameter	Value	Hyperparameter	Value
victim critic lr	=lr		
Hyperparameters for AMI			
Hyperparameter	Value	Hyperparameter	Value
p_ϕ lr	=lr	TAO lr	=lr
TAO critic lr	=lr	AMI lambda	.003

VII. Understanding the Variance of *Guo et al.*

In this section, we discuss the reason for the high variance of *Guo et al.* exhibited in MAMujoco environment, such that the high variance is not due to the use of our adversarial reward. We put forth three hypotheses:

- Hypothesis 1: the variance is due to the larger overall reward, since *Guo et al.* minimize victim reward and maximize adversary reward simultaneously. Under this reward, a learner can not converge to a good policy.
- Hypothesis 2: the variance is due to the use of victim reward, *i.e.*, some terms in victim reward will lead to high variance.

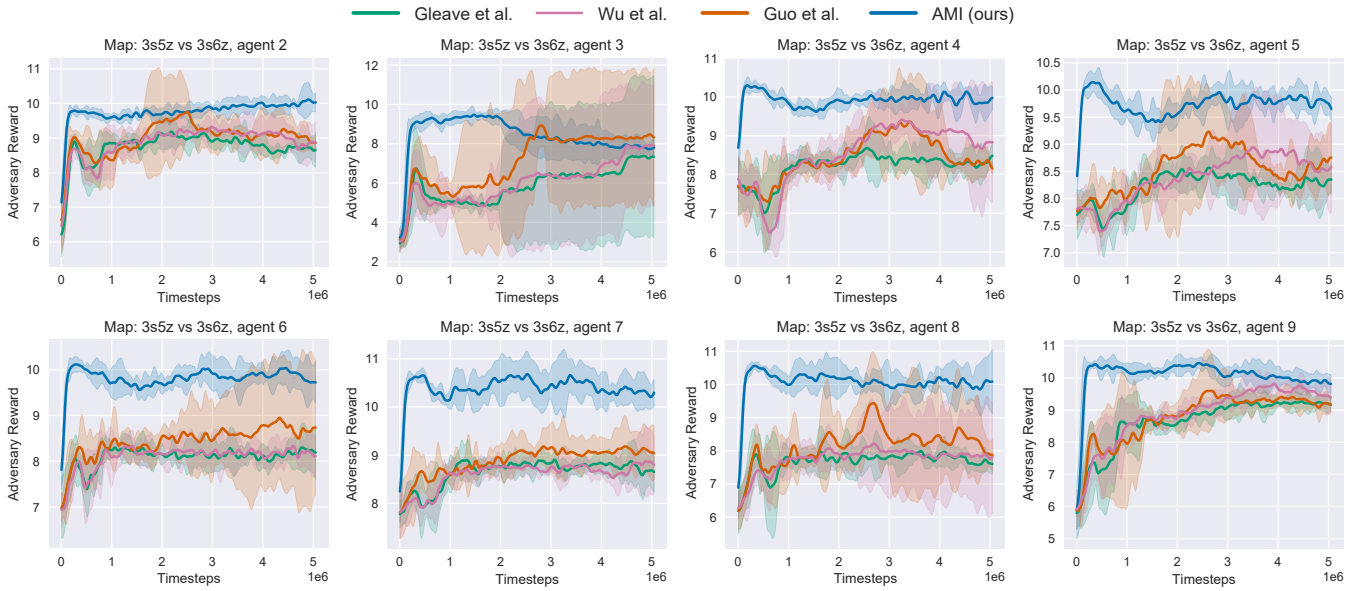

Fig. A4: Learning curves for AMI and baseline attack methods attacking agents with different IDs in *3s5z vs 3s6z* environment. The agent controlled by adversary can either be a stalker or a zealot, depending on IDs of the attacker. The solid curves correspond to the mean, and the shaped region represents the 95% confidence interval over 5 random seeds.

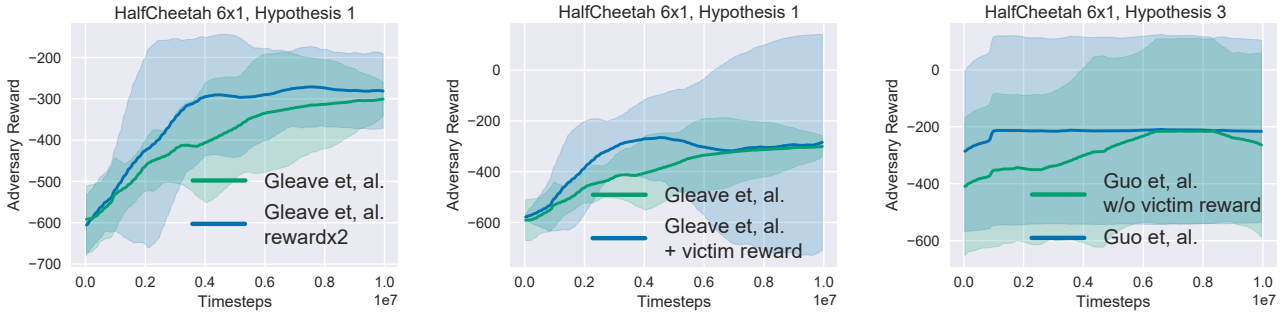

(a) Hypothesis 1 (b) Hypothesis 2 (c) Hypothesis 3

Fig. A5: Verifying the hypothesis of *Guo et al*. Our hypothesis 2 and 3 holds, which explains the high variance of *Guo et al.* is mainly due to their method and reward design.

- Hypothesis 3: the variance is due to the use of two critics, the method specifically proposed by *Guo et al*, such that the two critic structure intrinsically brings higher reward.

We verify the three hypothesis by experiments in Fig. A5. All experiments were conducted on *HalfCheetah 6x1*.

Hypothesis 1. We design experiment to verify our first hypothesis by experimenting on *Gleave et al.*. Since the method of *Guo et al.* is build on *Gleave et al.*, we use the method of *Gleave et al.* to disentangle the effect of reward and method. We conduct two experiments, (1) *Gleave et al.* using adversarial reward. (2) *Gleave et al.* using *doubled* adversarial reward. If larger reward impedes convergence, then *doubled* adversarial reward should exhibit higher variance. However, as shown in Fig. A5a, higher reward magnitude does not triggers higher variance.

Hypothesis 2. We continue on the method of *Gleave et al* and test if adding victim reward to total reward creates higher variance. As shown in Fig. A5b, our hypothesis holds, such that using victim reward will increase variance in some environments. We hypothesis this as a consequence of adding auxiliary reward terms (*i.e.*, *reward_ctrl*) in victim reward for victim training. These auxiliary reward can be useless in policy based attack, and thus increase variance. However, the variance after using negated victim reward is still not as large as exhibited in *Guo et al.*, showing the high variance also stems from other roots.

Hypothesis 3. Finally, we evaluate if using different reward in the method of *Guo et al.* reduce variance. As shown in Fig. A5b, even not using victim reward as stated in *Guo et al.*, their method still exhibits high variance. As a consequence, we hypothesis that the use of two critics that jointly updates adversary policy brings large instability, and is the main root of the variance in *Guo et al*. In contrast, our AMI use adversary reward only, and is of lower variance and better performance.

VIII. Analyzation of AMI policies in MAMujoco environment.

In this section, we analyze AMI policy in *MultiagentSwimmer 6x2* in MAMujoco environment. The behaviors are shown in Fig. A6. In this scenario, victims are rewarded by moving

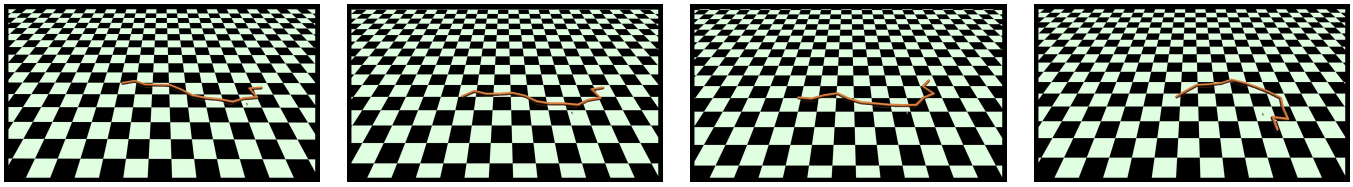

(a) Gleave et al. (b) Wu et al. (c) Guo et al. (d) AMI (ours)

Fig. A6: MAMujoco results under different attacks. While baselines physically interfere with victims, victims are still able to move in +x direction. In contrast, AMI fools victims towards jointly worst policy by fooling it to move clockwise.

along +x position as quick as possible. While the adversarial policy learned by *Gleave et al.*, *Wu et al.* and *Guo et al.* simply choose not to cooperate, the rest of the victims can still achieve the desired result under the attack. In contrast, our AMI attack learns to take actions that fool victims to move clockwise. In this way, victims are fooled to move towards a misleaded direction, resulting in joint failure.

IX. Statistical Tests of Real-World Environment

In this section, we provide more details of statistical tests in our experiments. Our experiment uses a *within-subject design* since the initialization is fixed for all baselines in the same runs. A nonsignificant Shapiro-Wilk W test for normality on adversary reward of all methods indicates that the data are normal (for *Gleave et al.*, mean=47.59, std=4.53, W=.97, p=0.93; for *Wu et al.*, mean=47.56, std=4.21, W=.93, p=0.46; for *Guo et al.*, mean=47.81, std=5.07, W=.93, p=0.42; for AMI, mean=53.24, std=2.81, W=.95, p=0.71;).

Since the data distribution does not violate a normal distribution, we use paired samples t-test to evaluate the statistical significance between AMI and all baselines. The improvement of AMI on adversary reward is significant comparing with all methods. Specifically, AMI is significant compared with *Gleave et al.*, (t(9)=-7.08, p<.001), *Wu et al.*, (t(9)=-6.83, p<.001) and *Guo et al.*, (t(9)=-4.01, p<.05).